PB-216 550

REMOVAL OF SUB-MICRON PARTICLES IN ACTIVATED CARBON FILTER BEDS

John Thomas Cookson, Jr.

Maryland University
College Park, Maryland

December 1968

DISTRIBUTED BY:

NTIS

National Technical Information Service
U. S. DEPARTMENT OF COMMERCE
5285 Port Royal Road, Springfield Va. 22151

WP-781

PB 216 550

ENVIRONMENTAL HEALTH ENGINEERING
CIVIL ENGINEERING DEPARTMENT
UNIVERSITY OF MARYLAND

RESEARCH ON

REMOVAL OF SUB-MICRON PARTICLES IN ACTIVATED CARBON FILTER BEDS

BY

JOHN THOMAS COOKSON

LIBRARY
FWPCA, Ohio Basin Region
4676 Columbia Pkwy. Cina, O. 45226

DECEMBER 1968

Reproduced by
NATIONAL TECHNICAL
INFORMATION SERVICE
U S Department of Commerce
Springfield VA 22151

PREPARED FOR

WATER POLLUTION CONTROL ADMINISTRATION

DEPARTMENT OF THE INTERIOR

UNITED STATES

92

REPORT

of

RESEARCH

on

REMOVAL OF SUB-MICRON PARTICLES IN ACTIVATED CARBON FILTER BEDS

* * * *

by

JOHN THOMAS COOKSON, JR.
Associate Professor of Civil Engineering

December 1968

ENVIRONMENTAL HEALTH ENGINEERING
CIVIL ENGINEERING DEPARTMENT
UNIVERSITY OF MARYLAND
College Park

I-a

Preface

This study was undertaken to provide a better understanding of colloid removal in filter beds. The influence of chemical and physical parameters are evaluated and a model presented to correlate physical filtration parameters to removal efficiency.

The removal of the virus Escherichia coli bacteriophage T_4 is studied in beds of activated carbon. It should be emphasized that this study has many ramifications, since it will apply to the removal of color and other organics by filtration units and adsorption beds.

The filtration mechanism is viewed as physical and chemical phenomena. The physical phenomenon depends on the transport of particles to be removed from the bulk flow to the surface of the filter medium, a transport step. The variables of flow rate, bed depth, void fraction, particle and bed characteristics, Reynolds number, Schmidt number, and virus removal are evaluated by mass transfer theories. The chemical phenomenon of filtration depends on the chemical interaction of the particle with the suspending solution and the filter medium, an attachment step. Thus, the chemical characteristics of the aqueous phase and the surface characteristics of the viruses and activated carbon medium are evaluated.

This report has been divided into three major parts, each related to a specific phase of the study. Part I presents

studies on the chemical nature and behavior of activated carbon in water. In Part II, the mechanism of virus adsorption on activated carbon is presented, and Part III deals solely with the physical aspects of filtration. A transport model, based on diffusional transfer in a flowing fluid, is correlated to experimental data.

Acknowledgments

The author acknowledges the valuable contributions of Mr. Charles R. Jones and Mr. Patrick M. Tobin for their laboratory assistance.

This investigation was initially supported by P. H. S. Research Grant and later by Federal Water Pollution Control Administration Research Grant No. WP-00981.

CONTENTS

PART I

Functional surface groups on activated carbon

Studies are presented on the chemical surface characteristics and behavior of activated carbon in water. The electrophoretic mobility of activated carbon is studied in solutions at varying ionic strength and pH. The negative charge of activated carbon increases with increasing pH. The charge is suppressed by salt ions, the divalent ions being more effective than the monovalent. Surface potential of activated carbon is determined by physical sorption of hydrogen and hydroxyl ions rather than ionization of acidic surface groups.

PART II

The mechanism of virus adsorption on activated carbon

Studies are conducted on the adsorption of Escherichia coli bacteriophage T_4 on activated carbon, and the physico-chemical groups involved in attachment.

Attraction is due to electrostatic forces between the virus and carbon. An optimum pH and ionic strength are displaced as a result of their influence on the electrostatic forces and configuration of viral tail fibers. Carboxyl or lactone groups on the carbon surface, and the virus's tail fibers are the likely groups involved in the attachment of virus to carbon. The active sites on activated carbon for adsorption of bacteriophage T_4 are completely blocked by methylation.

PART III

Application of mass transfer theory to filtration

Removal of the virus Escherichia coli bacteriophage T_4 is studied in packed beds of activated carbon. The chemical characteristics of the system are maintained at optimum conditions for virus attachment, while the physical characteristics are varied. Virus removal is interpretated by a physical model based on particle transport by diffusion in a flowing fluid.

Virus removal closely follows the transfer model, which can be used to predict the effects of flow rate, bed height, void volume, and bed grain size on removal efficiency.

PART I

FUNCTIONAL SURFACE GROUPS ON ACTIVATED CARBON

Filtration is often viewed as a physical phenomena with little or no regard to chemical interactions of the particles with the suspending solution and the filter medium. The chemical characteristics of the aqueous phase, and the surface characteristics of the suspended particles and filter medium must be considered in any filtration theory. Particle attachment depends on the surface chemistry of the respective materials, and the behavior of their surface properties in aqueous solutions. Double layer interactions and specific chemical interactions have been noted in removal of turbidity, hydrous ferric oxide and clay colloids by filter beds.

Activated carbon beds have been found more effective in removing viruses, organics responsible for taste and odor, and pesticides than sand beds. This phenomenon is not only a result of the greater surface area of activated carbon, but, more importantly, results from the chemical nature of the carbon's surface. Effective and efficient use of activated carbon in the form of suspension or packed bed necessitates an understanding of its chemical nature and behavior in water.

The pH of the suspending solution greatly affects both the rate at which colloids are sorbed and the total amount sorbed. A change in pH can cause (1) a change in net surface charge, effecting electrostatic interactions between the colloids and bed medium, and (2) a change in the degree

of ionization of surface groups which may chemically interact to bind the colloids to the filter bed. Removal of colloids by filtration requires that the colloids and filter medium make contact and then stick. Repulsive surface charges may hinder contact, and therefore cause inefficient filtration. Thus, knowledge was sought on the potential determining ions or groups on the activated carbon bed medium used in these studies. The surface charge of activated carbon was studied in solutions of varying ionic strength and pH by electrophoretic mobility techniques. The importance of surface oxides on establishing the surface potential was evaluated by electrophoretic mobility changes resulting from methylation and hydrolysis of these groups.

Surface Chemistry of Activated Carbon

The temperature and gases in which carbon is activated determines its surface characteristics. Base sorption on sugar, coconut shell and cotton stalk charcoals increases with increasing activation temperature up to 400°C, at which point it begins to decrease with increasing temperature. On the other hand, acid sorption decreases and reaches a minimum at 400°C, and then increases to a maximum when an activation temperature near 800°C is attained (1). Insight to the types of functional groups that can exist on the surface of activated carbon can be obtained by considering its molecular and crystalline structure. Because of random oxidation, the structure of activated carbon is disorganized more than that of graphite. The graphite crystal

is composed of layers of fused hexagons held approximately 3.35 Å apart by weak van der Waal's forces. The carbon layers are arranged so that one-half of the carbon atoms in any plane lie above the center of the hexagons in the layer immediately below it. Each carbon-carbon bond has a one-third double bond character. During carbonization, poly-nuclear aromatic nuclei are formed which are similar to, but much smaller than those found in graphite (2). X-ray spectrographs have shown that these nuclei are microcrystallites consisting of fused hexagonal rings of carbon atoms which are very similar to that of graphite (2) (Figure 1). The diameter of the planes making up the microcrystallite is estimated to be 150 Å and the distance between microcrystallites ranges from 20 to 50 Å. The oxidation proceeds to remove large portions of individual planes. The remaining fissures between parallel graphitic layers make up the macropores of activated carbon. These pores are generally less than 10 Å in width and make up most of the carbon's surface area. This surface area should be relatively free of attached functional groups since the planar surfaces are uniform in nature and the carbon's electrons are covalently bonded to surrounding carbon atoms. The edges of the microcrystallites are more heterogeneous than the planar surfaces. The carbon bonds at the edges are disrupted, yielding free valences which are very reactive and contain various types of functional groups.

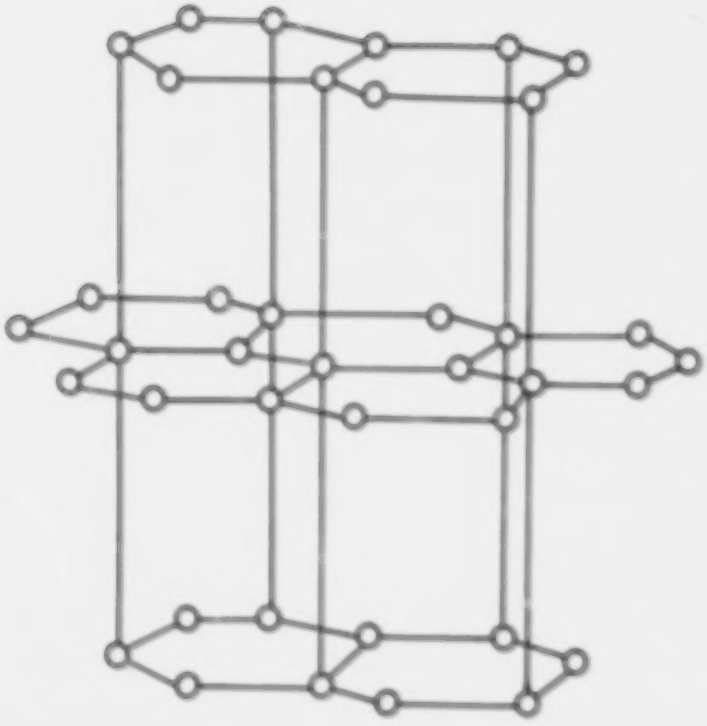

FIGURE 1. CARBON ATOM ARRANGEMENT IN A GRAPHITE CRYSTAL.

In activated carbon, oxygen generally constitutes 2 to 25 percent of the total carbon weight. An excellent discussion on the nature of surface oxides on activated carbon has recently been presented by Snoeyink and Weber (3). Carboxyl, carbonyl, f-lactone, n-lactone, phenolic, lactol, and quinone functional groups have been presented to explain the surface chemistry of activated carbon. Many of these groups have been indicated experimentally by direct titration, methylation, neutralization and infrared spectroscopy. Although much agreement on the nature of acidic groups on activated carbon exists among researchers, no quantitative information is available on these groups; and little information has been presented on the nature of basic groups. Acid sorption may be due to the presence of chromene-like structures on the carbon surface (4). Physical adsorption also has been proposed as the main force in binding acid.

Procedure

The carbon used in these studies was Nuchar C-190, a powdered carbon produced from the lignin fraction of wood by West Virginia Pulp and Paper Company. The salts of the lignin are first charred, thoroughly washed, and then given a series of activation treatments. The final activation treatment is with oxygen at approximately 490°C to 540°C. The approximate surface area as determined by nitrogen adsorption and the BET isotherm is 700-900 square meters per gram. Nuchar C-190 is reported to have the following percentages of total specific surface area present as oxygen-containing surface

groups: 0.36 carboxyl, 0.26 lactone, 1.06 quinone and 1.02 phenol (6).

Carbon of a small and uniform particle size was obtained by sieving. The carbon was washed and oven dried at 150°C. Stock carbon solutions were prepared and autoclaved for 15 minutes at 15 pounds per square inch pressure and 255°F. Autoclaving provided a better suspension of carbon by reducing flotation of the particles. The process is thought to expel gases from the carbon and to cause better wetting of the carbon surface.

The mobility of carbon particles was measured with microelectrophoretic equipment consisting of:

1. Binocular microscope with dark field condenser.
2. Briggs cell.
3. Heathkit Regulated Power Supply, Model 1P-32.
4. Heathkit Impedance Bridge, Model 1 B-2A.
5. Conductivity cell.
6. Simpson Milliammeter, Model 373.

The Briggs cell and electrical equipment were utilized as outlined by Black (5). Three different sets of 10 particles each were timed for each test solution. Carbon particles of approximately 3.5 microns were selected visually for timing by using a Proton graticule.

Experimentation

Mobility tests were conducted on untreated carbon particles suspended in ten test solutions of ionic strength 0.10, buffered at pH values from 2.4 to 10.8 (Table 1). The ionic strength of all test solutions was composed primarily

of sodium and chloride ions to minimize the effect of different buffers. However, no significant change in the mobility of the carbon particles was noted when suspended in two different buffer systems of KH_2PO_4 - NaOH and $Na_2B_4O_7$-HCl (Table 1).

The effect of pH on the mobility of carbon particles is greatest at pH values below 5 and above 8. Little effect can be noted in the pH range 5 through 8, as shown by the flat slope of the mobility versus pH plot (Figure 2). The negative mobility of carbon increased with pH, indicating a net increase in negative charge. This charge could result from the ionization of carboxyl and phenolic acidic surface groups on the carbon surface. As pH increased, the presence of negatively charged COO^- ions would increase and cause a greater negative mobility. The above interpretation of pH effect on mobility, however, appears to be incorrect. As discussed below, methylation of acidic surface groups on carbon did not measurably affect the carbon's mobility.

Another explanation for the increase in mobility with pH is specific sorption of hydroxyl and hydrogen ions on the carbon surface. The presence of chromenes on carbon will also cause the carbon surface to become less negative in acid solution, resulting in a sharp decrease in mobility, with decreasing pH. In acid, chromenes may cause the carbon to have a net positive charge; however, positively charged particles were not noted in the pH range studied (Figure 2).

The effect of ionic strength on mobility of untreated carbon was determined at a pH near 6.0. Ionic strength was

TABLE 1

TEST RESULTS OF pH EFFECT ON THE MOBILITY OF CARBON PARTICLES

pH	Buffer System	Ionic Strength			Mobilities μ/sec/v/cm
		Buffer	NaCl	Total	
2.4	KCl-HCl	0.019	0.081	0.100	0,0,0
3.0	KHP-HCl	0.017	0.083	0.100	-1.1 -1.1 -1.1
4.0	KHP-HCl	0.021	0.079	0.100	-1.3 -1.2 -1.2
5.0	KHP-NaOH	0.022	0.078	0.100	-1.7 -1.7 -1.7
6.0	KH_2PO_4-NaOH	0.022	0.078	0.100	-2.0 -1.8 -1.7
7.0	KH_2PO_4-NaOH	0.028	0.072	0.100	-1.7 -1.8 -1.9
8.25	$Na_2B_4O_7$-HCl	0.027	0.073	0.100	-2.0 -1.9 -1.9
8.8	$Na_2B_4O_7$-HCl	0.029	0.071	0.100	-2.2 -2.1 -2.2
9.8	$Na_2B_4O_7$-NaOH	0.014	0.086	0.100	-2.6 -2.5 -2.5
10.8	$NaHCO_3$-NaOH	0.020	0.080	0.100	-2.9 -2.8 -2.9
8.7	KH_2PO_4-NaOH	0.030	0.070	0.100	-2.3 -2.3 -2.4
8.8	$Na_2B_4O_7$-HCl	0.027	0.073	0.100	-2.4 -2.5 -2.4

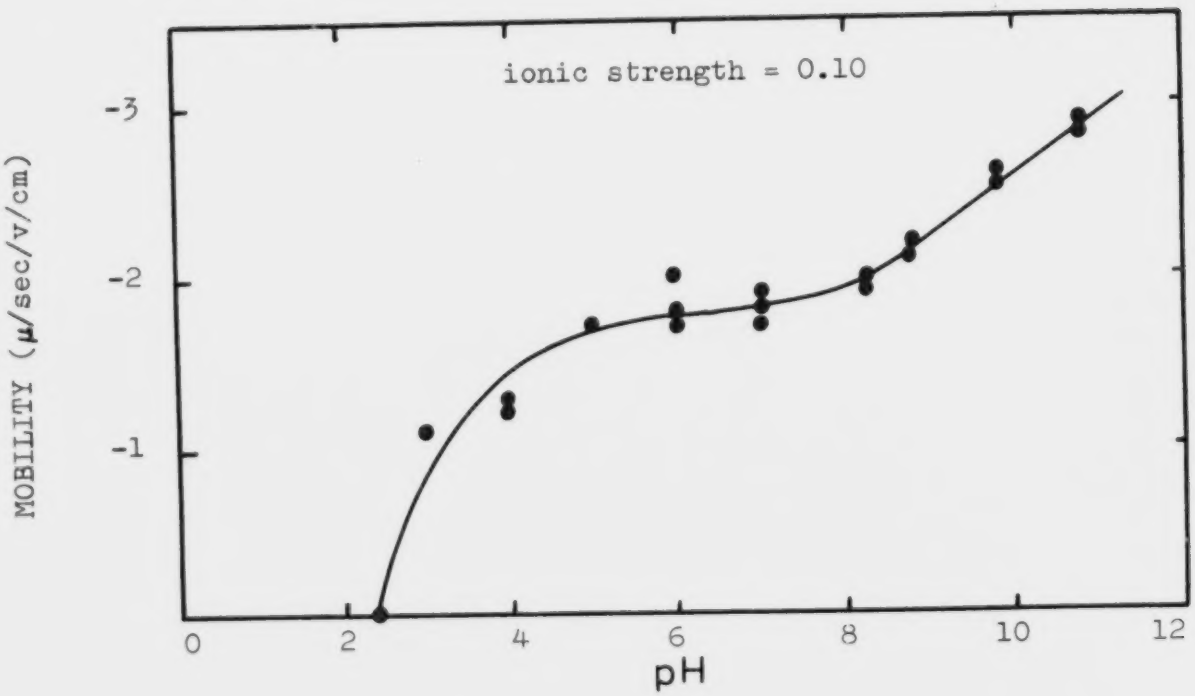

FIGURE 2. VARIATION OF MOBILITY WITH pH FOR UNTREATED CARBON PARTICLES

maintained exclusively with NaCl, except where otherwise indicated. The negative mobility of carbon particles decreased with an increase in the ionic strength of the solution (Figure 3). The large number of ions at the higher ionic strengths may shift the ionization equilibrium of the proposed surface groups on the carbon. This effect, however, is insignificant compared to the compression of the double layer. The compression of the double layer has previously been shown to be the reason for a decrease in zeta-potential with increasing ionic strength. The mobilities of the carbon suspended in the $BaCl_2$ solutions are considerably lower than those of the carbon suspended in NaCl solutions (Figure 3). The observed difference between Na^+ ion and Ba^{++} ion is in agreement with the Schulze-Hardy rule, which accounts for the valence difference of counterions on flocculation of colloidal particles.

The importance of surface oxides on activated carbon in explaining the pH effect on mobility was investigated by chemically treating the carbon. Carbon was reacted with diazomethane to methylate carboxyl, f-lactone and phenolic groups, and with HCl-methanol to methylate only carboxyl groups on the carbon's surface. The carbon was also reacted with concentrated propylene oxide to form esters with carboxyl surface groups. An ether solution of diazomethane (CH_2N_2) generally reacts with carboxyl acid groups to form hydrolyzable methyl esters, and with phenolic groups to form non-hydrolyzable methyl ethers (4). Diazomethane also

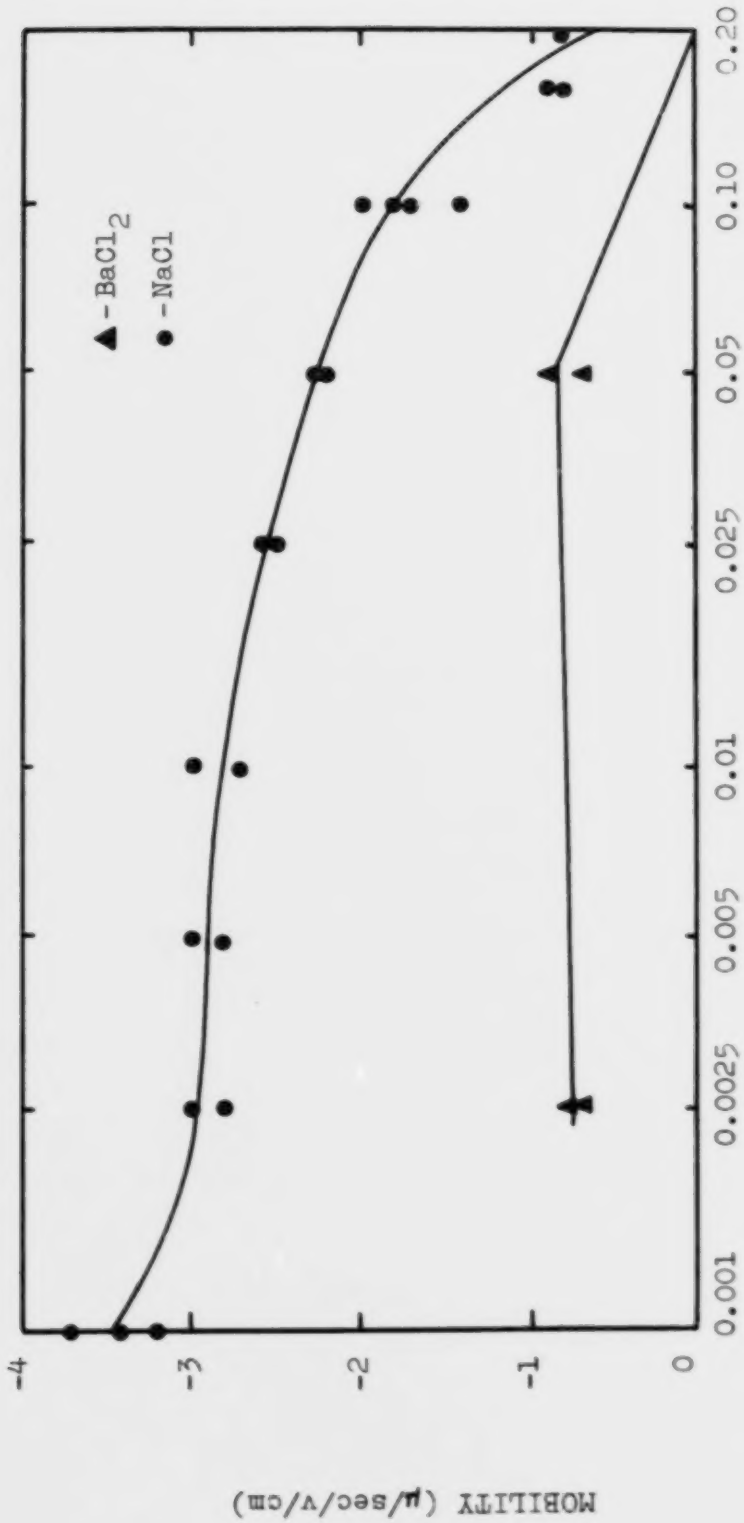

FIGURE 3. VARIATION OF MOBILITY WITH IONIC STRENGTH FOR UNTREATED CARBON PARTICLES

reacts with fluorescein type lactones forming the quinoid type lactones (4):

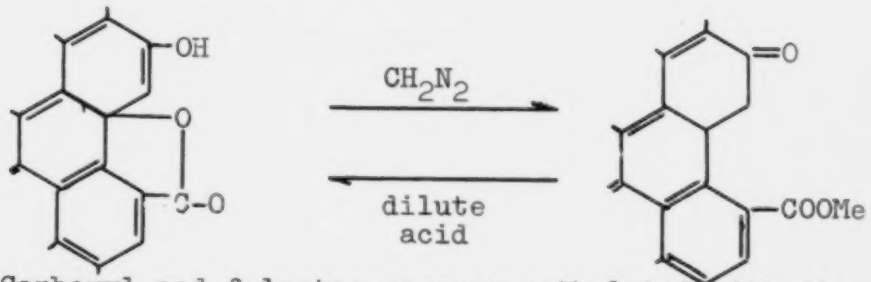

Carboxyl and f-lactone groups methylated with diazomethane will hydrolyze in dilute HCl to form the original carboxyl and f-lactone groups.

An ether solution of diazomethane was prepared following the method of Gattermann and Wieland (7). Thirty milliliters of cold, 40% KOH were mixed with 100 milliliters of pure diethyl ether and placed in an ice bath. Ten grams of nitrosomethylurea ($CH_3N(NO)CONH_2$) were slowly added while mixing. After the reaction was complete (5-10 minutes), the deep yellow solution of diazomethane was decanted from the residual solution and stored at -20°C. The yield was approximately 100 ml. of ethereal diazomethane. Exactly one gram of untreated carbon was reacted with 20 ml. of ethereal diazomethane solution for approximately five days at 5°C, with 5 more ml. of diazomethane added to each flask on the second day. After five days, each sample of reacted carbon was individually filtered from the diazomethane with a millipore filter and washed with approximately 150 milliliters of diethyl ether to remove any residual diazomethane.

Hydrolysis of the methylated surface oxides was performed by treating the diazomethane reacted carbon with hot 0.1N HCl for one hour. For the HCl-methanol treatment, powdered carbon was suspended in 0.1N HCl in absolute methanol for 2 days at 25°C. For the propylene oxide treatment, carbon was reacted with concentrated propylene oxide for 2 1/2 days at 25°C. Carbon treated by the above procedures was filtered and repeatedly washed until no measurable trace of the reacting solution was noted in the washings. The carbon was then oven-dried for three hours at 105°C and stored in tightly stoppered bottles.

Base and acid neutralization capacity of carbon was determined to evaluate the effect of the above chemical treatments on carbon surface groups. Boehm (4) has shown that $NaHCO_3$ neutralization is caused by carboxyl groups, Na_2CO_3 neutralization by carboxyl and f-lactone groups and NaOH neutralization by carboxyl, f-lactone and phenolic groups. Carboxyl groups are believed to constitute the hydrolyzable methoxy content, and phenolic groups the non-hydrolyzable methoxy content.

Treated and untreated carbons were reacted with NaOH, Na_2CO_3, $NaHCO_3$ and HCl to determine the amount of base and acid consumed by the carbon. In each test, a given weight of carbon was added to 40 ml. of base, using 0.025N or 0.05N solutions. In all cases, blanks were run without carbon. The carbon was filtered from each basic solution after reacting for sixteen hours at 25°C, and the filtrates

were titrated with 0.1N or 0.025N HCl. A titration endpoint of 8.3 was used for the NaOH and 4.0 for the Na_2CO_3 and $NaHCO_3$. The milliequivalents of base neutralized per gram of carbon was determined from these titration results.

The average neutralization values for Nuchar C-190 are 0.096, 0.133, and 0.312 milliequivalents per gram for $NaHCO_3$, Na_2CO_3 and NaOH, respectively (Table 2). As noted above, $NaHCO_3$, Na_2CO_3 and NaOH should neutralize carboxyl groups, carboxyl and f-lactone groups, and carboxyl, f-lactone and phenolic groups, respectively. In view of this, 0.096, 0.037, 0.179 milliequivalents of carboxyl, f-lactone. and phenolic groups, respectively, exist per gram of carbon.

The acid neutralization capacity of carbon was determined by reacting 4.0 grams of carbon with 100 ml. of 0.05N HCl for 17 hours. The carbon was then filtered through a millipore filter and the filtrate titrated with 0.05N NaOH. Neutralization of HCl amounted to 0.28 milliequivalents per gram of carbon (Table 2). Total acid adsorption cannot be attributed to genuine surface groups of basic nature. Adsorption of protons by physical forces and secondary adsorption of anions will also occur. Carbon that had adsorbed protons was separated by filtration and resuspended in basic solutions to study hydrogen ion elution (Table 3). It was found that only 0.006 meq/gm of free acid (that is, acid not sorbed on the carbon) was carried over with carbon in these elution tests. After shaking for 12 hours, 0.019 milliequivalents of acid per gram of carbon desorbed into

TABLE 2

SUMMARY OF ACID AND BASE NEUTRALIZATION CAPACITY OF UNTREATED AND TREATED CARBON

Treatment	Average Acid and Base Neutralized (meq/GRAM)			
	HCl	$NaHCO_3$	Na_2CO_3	NaOH
None	0.280	0.096	0.133	0.312
Methanol-HCl (I)	--	0.224	0.256	0.416
Methanol-HCl (II)	--	0.168	0.280	0.456
Propylene Oxide	--	0.064	0.128	0.272
Diazomethane (I)	--	-0.088	-0.104	0.192
Diazomethane (II)	--	-0.108	-0.072	0.168
Hydrolyzed Diazomethane (I)	--	0.112	0.176	0.368

Note: The negative sign indicates the milliequivalents of hydrogen ion per gram of carbon that was neutralized in the basic solutions. No base was neutralized. The acidity of the solution decreased.

TABLE 3

ELUTION OF ADSORBED PROTONS FROM CARBON

Elution Solution	Acid Desorbed meq/Gram
water	0.019
$NaHCO_3$	0.083
Na_2CO_3	0.127
NaOH	0.107

distilled water (Table 3). When this same carbon was suspended in basic solutions, a total of 0.083, 0.127, and 0.107 meq/gm was desorbed in $NaHCO_3$, Na_2CO_3, and NaOH, respectively. Thus, all adsorbed hydrogen ions are not attached to sites on the carbon surface with equal bonding strength.

Carbon was reacted by separate procedures with HCl-methanol reagent and labeled I and II in Table 2. The neutralization of base by the treated carbon was larger in both cases than that for untreated carbon. A lower capacity would be expected since carboxyl groups will methylate according to the equation:

The explanation appears to be adsorption of protons on the carbon during the HCl-methanol treatment. These adsorbed protons would not wash off with distilled water but were eluted by the bases. Adsorption of protons also was found when the methylated carbons were hydrolyzed with HCl. The hydrolyzed carbons had a greater base neutralization capacity than before methylation (Table 2).

Propylene oxide will esterify carboxyl groups according to the following equation:

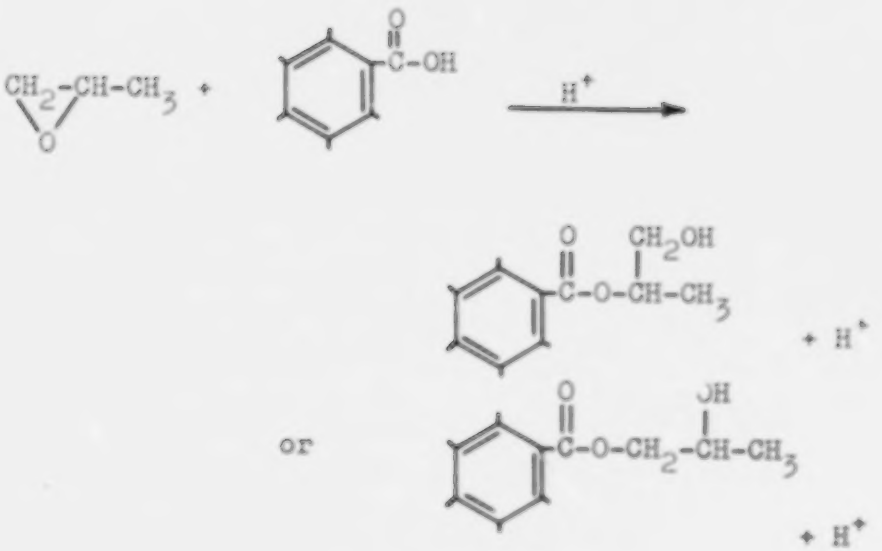

Two samples of carbon were treated with propylene oxide as outlined above and reacted with each of three bases - $NaHCO_3$, Na_2CO_3 and NaOH. The milliequivalents of base neutralized after 16 hours of carbon contact was determined as before (Table 2). The neutralization values for $NaHCO_3$, Na_2CO_3, and NaOH were 0.032, 0.005, and 0.040 milliequivalents, respectively, lower than those values for untreated carbon. Thus, approximately 0.04 milliequivalents of acidic surface groups were esterified by propylene oxide per gram of carbon.

Diazomethane will form methoxy groups with carboxyl, phenolic, and f-lactone groups. Since the methoxy groups remained unionized in solution, their presence should decrease the base consuming capacity of the carbon. Two preparations of carbon treated by diazomethane (I & II) were made and tested for base neutralization. The normalities of the $NaHCO_3$ and Na_2CO_3 solutions after reacting with the methylated carbon were higher than the initial normalities by the

amount of the negative neutralization values indicated in Table 2. Carbon methylated with diazomethane was also shaken with distilled water to observe any hydrogen ion adsorption on the carbon from the water. Four hundredths (0.04) of a milliequivalent of hydrogen ions adsorbed on the carbon. Since diazomethane treatment only ties up base neutralizing groups on the carbon, hydrogen ions will still be sorbed by the carbon, thereby increasing the basic normality of the test solutions. Hydrogen ions will have less tendency to adsorb on carbon suspended in a strong base, such as NaOH, than in weak bases, such as $NaHCO_3$ and Na_2CO_3. This condition was found for both diazomethane treatments of carbon (Table 2). The normality of the $NaHCO_3$ solution increased more than the Na_2CO_3 solution. In the stronger base of NaOH, hydrogen ion adsorption was not great enough to offset the NaOH neutralized by acidic groups on the carbon that resisted methylation.

The NaOH neutralizations for the diazomethane treated carbon I and II were 0.120 to 0.144 milliequivalents per gram lower than that for the untreated carbon, indicating that 0.120 to 0.144 milliequivalents of acidic groups are methylated per gram of carbon (Table 2). Carboxyl, f-lactone and phenolic groups apparently are not the only acidic groups on the carbon's surface, since the total 0.312 milliequivalents of acidic groups per gram of carbon were not methylated by diazomethane. The 0.168 milliequivalents per gram which was not methylated by diazomethane may be acidic groups

such as a normal lactone, or may result from physical adsorption of hydroxyl ions.

Mobility Results

In the pH range 9.7 to 9.8, many acidic groups on activated carbon are ionized; however, no mobility difference was noted between the untreated carbon and that methylated with the HCl-methanol and diazomethane reagent (Table 4). The lower mobility of the hydrolyzed carbon at a pH of 9.7 is probably due to the adsorbed protons as noted by the neutralization tests (Table 2). At a pH of 6.8 to 7.0 the mobilities of the methylated carbons were slightly greater than the untreated carbon, and, for the pH values of 3.0 and 5.9, the mobilities of the methylated carbons were slightly less than the untreated carbons. These differences are probably insignificant. A change in mobility of 0.4μ/sec/v/cm was estimated significant for the techniques employed.

Calculations are presented below to indicate the change in surface potential needed to cause a corresponding change in mobility of 0.4μ/sec/v/cm. Although any quantitative evaluation of a corresponding change in surface potential is impossible, an indication of the surface potential can be computed from the Gouy theory. From the Gouy theory, the decay of potential with distance for a given surface potential and a given electrolyte concentration, as based on a single flat double layer, is given by:

TABLE 4

COMPARISON OF THE MOBILITIES OF UNTREATED CARBON AND TREATED CARBON

Treatment of Carbon	pH	Ionic Strength	Number of Tests	Average Mobility μ/sec/v/cm
Untreated	9.8	0.1	30	2.5
Methanol-HCl	9.7	0.1	30	2.5
Diazomethane	9.8	0.1	60	2.5
Hydrolysis-Diazomethane	9.7	0.1	30	2.2
Untreated	7.0	0.1	30	1.8
Diazomethane	6.9	0.1	60	2.1
Hydrolysis-Diazomethane	6.9	0.1	30	2.1
Untreated	5.9	0.1	30	1.8
Propylene Oxide	5.9	0.1	30	1.6
Untreated	3.0	0.1	30	1.1
Methanol-HCl	3.0	0.1	30	1.3
Diazomethane	3.0	0.1	40	0.8
Hydrolysis-Diazomethane	3.0	0.1	30	1.0

$$e^{y/2} = \frac{e^{z/2} + 1 + (e^{z/2} - 1)e^{-\beta}}{e^{z/2} + 1 - (e^{z/2} - 1)e^{-\beta}}$$

Where:

$y = ve\rho/kT$

$z = ve\Phi_o/kT$

$\beta = Kx$

v = valence

k = Boltzmann constant

T = absolute temperature

Φ_o = surface potential

ρ = Zeta potential at a distance x from the surface

x = distance from the surface

e = elementary charge 4.80×10^{-10} esu

and $1/K$ = thickness of the double layer

The thickness of the double layer is described by

$$1/K = \left[\frac{Dkt}{8\pi ne^2v^2}\right]^{1/2}$$

Where: D = Dielectric constant = 80

n = (normality $\times 10^{-3}$ x Avogadro's number) ions/cm^3

= N $\times 10^{-3} \times 6.02 \times 10^{23}$ ions/cm^3

Mobility (m) in μ/sec/v/cm is related to zeta potential (ρ) in millivolts at some distance x from the surface by the expression:

$$\rho = 14.2 \text{ mv}$$

for water at 20°C. Zeta potential is the potential at the

shear plane; however, this distance, x, is unknown and the calculations below are made for x equal to the thickness of the double layer, 1/K, and the thickness of the Stern layer.

For a typical mobility test where ionic strength equals 0.10 (for a monovalent ion $n=6.02 \times 10^{19}$ ions/cm^3), mobility equals 1.85 μ/sec/v/cm (for activated carbon at pH 7.0), and kT equals 4.0×10^{-12} ergs at room temperature, the zeta potential (ζ) is 26.2 mv and the thickness of the double layer (1/K) is 9.58Å. The thickness of the Stern layer is equivalent to two monomolecular layers of adsorbed water, or 5 Å. If the shear plane occurs at a distance equal to 1/K, than from the above equations

$$y = 1.05 \text{ ergs/mv}$$

$$z = 1.2 \times 10^4 \, \Phi_o \text{ ergs/mv}$$

$$\beta = 1$$

and

$$e^{0.523} = \frac{e^{z/2}(1 + e^{-1}) + 1 - e^{-1}}{e^{z/2}(1 - e^{-1}) + 1 + e^{-1}}$$

solving for Z:

$$Z = 3.48$$

therefore: $\Phi_o = 87.0$ mv

For a mobility reduction of 0.4 μ/sec/v/cm, the corresponding zeta potential is reduced to 20.6 mv.

Solving for the new surface potential, one obtains

$$\Phi_o = 61.5 \text{ mv}$$

Therefore, a change in mobility of 0.4 μ/sec/v/cm will correspond with an approximate change of 29 percent in surface potential.

Assuming the shear plane at the Stern layer, one obtains:

For ρ = 26 mv

and β = 0.522

Φ_o = 46.3 mv

For ρ = 20.6

and β = 0.522

Φ_o = 36 mv

Therefore, a change in mobility of 0.4 μ/sec/v/cm will correspond with an approximate change of 22 percent in surface potential.

These calculations illustrate that approximately a 20 to 30 percent change in the carbon's surface potential would be necessary to obtain a measurable change in mobility.

Conclusions

Activated carbon (Nuchar C-190) has approximately equal capacity to neutralize strong acid (0.280 milliequivalents of HCl per gram) and strong base (0.312 milliequivalents of NaOH per gram). Neutralization of base is not entirely due to the presence of carboxyl, f-lactone and phenolic groups. After methylation of these groups, the base neutralization capacity of carbon is reduced by only 46 percent. The other 54 percent may result from other acidic groups, such as normal lactones. Acidic surface groups, however, do not account for all of the neutralization phenomenon, since physical adsorption of hydrogen and hydroxyl ions occur. Hydrogen bonding with oxygen and nitrogen groups may occur

on the carbon surface. Adsorbed hydrogen ions are not completely eluted by water, but more elution is achieved in bases of increasing strengths.

Reliable results were not obtained on methylation of acidic groups by methanol and acid. The adsorption of hydrogen ions on carbon during the methylation process prevented evaluation of methylation success by base neutralization techniques. Hydrogen ion adsorption also made the results on hydrolysis of the methylated groups questionable. Methylation of the acidic surface groups on carbon did not cause a significant decrease in mobility. No more than 20 to 30 percent of the surface potential of activated carbon can be due to the ionization of acidic surface groups. The major contribution to surface potential is probably due to potential determining ions of hydrogen and hydroxyl. The charge on activated carbon varied from zero at pH 2.4 to increasing negative values with higher pH. In accordance with the Schulze-Hardy rule, divalent ions are more effective than monovalent ions in masking the change on carbon.

REFERENCES CITED

1. Puri, B. R., Singh, D. D., Nath, J. and Sharma, L. R., "Chemi-sorption of Oxygen on Activated Charcoal and Sorption of Acids and Bases", Industrial Engineering Chemistry, Vol. 50, July, 1958, p. 1071.

2. Wolff, W. F., "A Model of Active Carbon", Journal Physical Chemistry, Vol. 63, May, 1959, p. 653.

3. Snoeyink, V. L., and Weber, W. J., Jr., "The Surface Chemistry of Active Carbon", Environmental Science and Technology, Vol. 1, March, 1967, p. 228.

4. Boehm, H. P., "Chemical Identification of Surface Groups", Advances in Catalysis, Vol. 16, edited by D. D. Eley, H. Pines, and P. B. Weisz, Academic Press, New York, N. Y., 1966.

5. Black, A. P., and Smith, A. L., "Determination of the Mobility of Colloidal Particles by Microelectrophoresis", Journal American Water Works Association, Vol. 54, August, 1962, p. 926.

6. Questionnaire and Correspondence from West Virginia Pulp and Paper Company, 1968.

7. Gattermann, L., and Wieland, H., Laboratory Methods of Organic Chemistry, Macmillan and Co., London, England, 1948.

PART II

THE MECHANISM OF VIRUS ADSORPTION ON ACTIVATED CARBON

Introduction

The need of processes for removal or inactivation of water-borne viruses has been demonstrated beyond question by their transmission in drinking water and polluted streams. Animal viruses have been found in effluents and distribution systems that carry supposedly purified drinking water. Because of the decrease in available water supplies, the potential health hazard of viral pollution is increasing, and more knowledge on the survival and removal of viruses in sewage treatment and water purification processes is needed.

Activated carbon is recognized as a useful sorbent for removing organics and other specific compounds from water. Understanding the mechanism by which organics are removed from water by activated carbon is important in optimizing its use. This study provides some insight to the mechanism by which viruses, which behave as typical proteins in water, are removed by activated carbon.

Most viruses in water can be adsorbed or trapped by larger particles. This phenomenon has prevented the development of quantitative assays for viruses in waste water and natural water. Limited studies have been performed on virus adsorption on kaolin, aluminum hydroxide, zinc hydroxide, sand and carbon. Pyl (1) and Bush (2) mixed solutions of foot and mouth disease virus with animal charcoal. The carbon adsorbed the virus and, after inoculation into guinea pigs, release occurred causing infection. More recently,

activated carbon has successfully adsorbed polio virus and infectious hepatitis virus (3).

The author has previously reported studies on the kinetics and equilibria of virus adsorption on activated carbon (4). A diffusion limited model based on the von Smoluchowski equation with a Langmuir isotherm boundary condition was applied to the adsorption system (5). The present communication will be concerned with the mechanism of virus adsorption on activated carbon and the nature of the viral attaching groups and carbon sites.

Viruses are colloidal in size and generally range from 20 to 200 millimicrons (exceptions include members of the pox virus family). The surface characteristics of colloidal particles largely determine their behavior in solution. Viruses, therefore, behave as proteins, even though the internal structure may be non-protein in character. In their electrokinetic properties, viruses behave as amphoteric electrolytes. The net charge depends on solvent pH. The isolectric point differs among viruses. It occurs below pH 4.2 for E. coli bacteriophage T_2, at pH 3.9 for adenovirus M-2, and at pH 6 for foot and mouth disease virus. Most viruses display a net negative charge within the range of pH stability.

Materials

Activated carbon used in these experiments was West Virginia Pulp and Paper Company's Nuchar C-190, fractionated to a geometric mean diameter of 2.5 microns and a standard

deviation of 2.0. The average surface area was 1 square meter per gram assuming spherical particles (4). The specific surface of Nuchar C-190 was 700-900 m^2/gm. based on nitrogen adsorption and application of the Brunauer-Emmett-Teller (Bet) isotherm (6). Total pore volume was 0.9 cc/gm. Pore-size distribution for Nuchar C-190 was not available. It was assumed, however, to resemble typical activated carbons of similar specific area and total pore volume. Pore diameters greater than 1,200 Å contribute very little to total pore volume (7). Average pore diameters of 20 Å for activated carbon are expected from the concept of platelet structure. Carbon was washed in deionized water to remove dust and was dried in thin layers at 105°C for 24 hours. Stock suspensions at 200 mg/l in deionized water were autoclaved and stored at 4°C.

A bacteriophage was used, since assay techniques and knowledge of phage properties are more advanced for bacterial viruses than animal viruses. Both bacterial and animal viruses exhibit similar adsorption characteristics on host cells. Escherichia coli bacteriophage T_4 was selected because of its stability under adverse conditions and ease of assaying. An electron micrograph and the properties of Escherichia coli bacteriophage T_4 are given in Figure 1 and Table 1. E. coli B cells were used as hosts. Stock solutions of the virus were prepared and assayed by the plaque assay method. The virus and assay procedures were obtained from Dr. Robert S. Edgar of the California Institute of Technology and have previously been described in detail (4).

Methods

Adsorbent and virus were continuously mixed by a Gyrotary incubator shaker at constant temperature in 125-ml glass flasks. Reaction solutions of known chemical composition were made by adding stock solutions to deionized water. All stock chemical solutions and deionized water were autoclaved and stored at 4°C.

One-tenth milliliter samples were removed from the reaction solution and immediately diluted in 9.9 ml tryptone broth. If adsorbent was present, it was allowed to settle before sampling. Controls with adsorbents were run in all cases at identical temperatures, virus concentrations, and chemical compositions. Reaction solutions were buffered with potassium phosphate except as noted. The ionic strength was adjusted to the desired level by varying buffer strength and by sodium chloride.

Effect of pH on Adsorption

Since net charges on viruses are greatly influenced by the acidity of the surrounding solution, adsorption of virus to activated carbon was studied under six different hydrogen-ion concentrations at a constant ionic strength of 0.1. In each test, the buffer system was mono- and dipotassium phosphate with sodium chloride as necessary. Extreme pH values were attained with stock solutions of 0.1 N HCl and 0.1 N NaOH.

To compare the effect of pH on adsorption, the forward rate constant for each test was determined. Kinetic plots of

Figure 1. Electron micrograph of Escherichia coli bacteriophage T_4
(Approximate magnification of this electron micrograph: 3.4×10^5; negative stain; provided by Robert S. Edgar, California Institute of Technology)

Preceding page blank

TABLE 1

PROPERTIES OF ESCHERICHIA COLI BACTERIOPHAGE T_4

Size	
Head	65 x 80 millimicrons
Tail	100 x 20 millimicrons
Diffusion constant	
at 20°C	0.8×10^{-7} cm^2/sec
Specific weight	3.3×10^{-16} gm per particle

the data were made in the form of the reversible second-order equation as given below:

$$tk_1m = \ln\left[\frac{0.5(a_o + b_o + K^{-1} + m) - X}{0.5(a_o + b_o + K^{-1} - m) - X}\right]\left[\frac{a_o + b_o + K^{-1} - m}{a_o + b_o + K^{-1} + m}\right] \quad (1)$$

where:

a_o = initial concentration of virus (viruses/ml)

b_o = initial concentration of carbon sites (sites/ml)

t = time (sec)

k_1 = forward rate constant (ml/virus-sec)

k_2 = reverse rate constant (1/sec)

K = equilibrium constant ($K = {}^{k_1}/_{k_2}$)

x = concentration of adsorbed virus at time t (virus/ml)

$m = [(a_o - b_o)^2 + K^{-1}(2a_o + 2b_o + K^{-1})]^{1/2}$

The author has previously shown that adsorption of Escherichia coli bacteriophage T_4 to activated carbon can be represented by reversible second order kinetics (4) (5). Equilibrium studies with this virus and carbon gave values of 1.9×10^9 sites/mg and 4.0×10^{-7} ml/virus particle for carbon capacity and equilibrium constant, respectively (4). All of the results plotted as a straight line, as shown by the typical plot in Figure 2. Rate constants were determined from slopes of the kinetic plots and a significant effect of pH on adsorption was found (Figure 3). The forward rate constant is maximum at pH 7 and drops off to zero below pH 4.5 and above pH 10.

The main groups on viruses that can be affected by pH are the free side chains of amino acids. The amino-acid composition of bacteriophages T_2 and T_3 has been accurately determined (8), and should be similar to that of T_4. The important ionizable groups are amino, carboxyl, guanidino, imidazolyl, and sulfhydryl. About 80 percent of these ionizable groups are amino and carboxyl, indicating their probable importance over others in explaining the pH effect.

The adsorption rate falls to zero at pH values beyond the limit at which the amino and carboxyl groups ionize when incorporated in protein. The pH curve also rules out the possibility of significant participation by ionized forms of sulfhydryl (pK = 9), guanidino (pK = 12.5), and phenolic (pK = 10.1) groups since the pK values are incompatible with points of maximum pH effect. Although the imidazolyl group has a more compatible pK of 6, it constitutes only two percent of the amino acid-side chains.

The surface charge on activated carbon is also greatly influenced by pH. Electrokinetic studies were made on Nuchar C-190 using a Briggs cell in the manner reported by Black (9). Mobility of small carbon particles (about 1 micron) was measured in buffered solutions of constant ionic strength. The various buffers did not affect mobility of the carbon at identical pH values. The net negative charge on activated carbon was found to decrease with decreasing pH (Figure 4). Zero mobility was noted at pH 2.5.

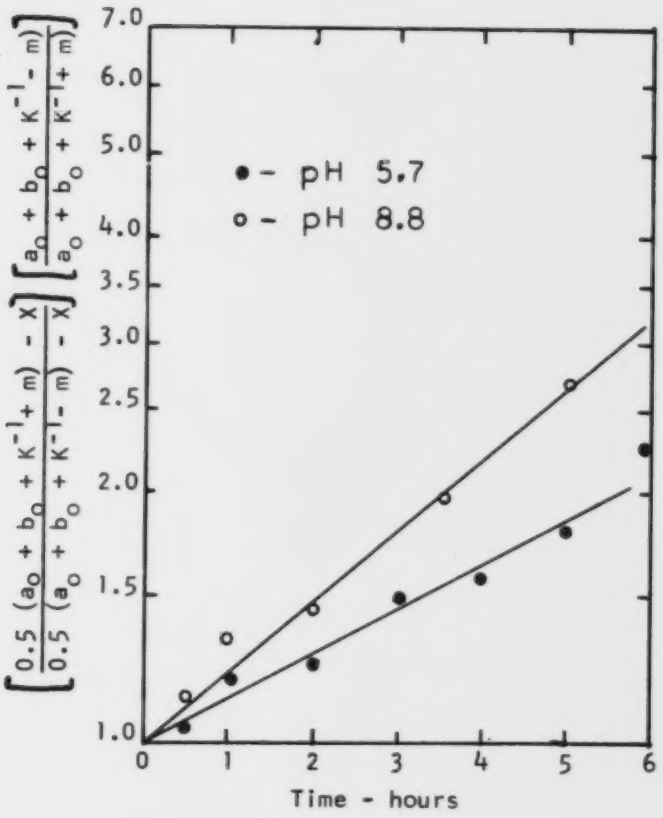

Figure 2. Reversible second-order kinetic plot of adsorption of T_4 phage on carbon at pH 5.7 and 8.8.

Figure 3. Forward Rate Constant (k_1) vs. pH for adsorption of T_4 phage on carbon

The effect of pH on adsorption of viruses to activated carbon resembles effects found during adsorption of viruses to host cells. The pH effect can be explained if amino groups on the virus interact with carboxyl groups on the activated carbon. Adsorption is decreased at low pH levels since the carboxyl groups are not ionized. At high pH values, the activated carbon and virus are negatively charged. At about pH 7, positively charged amino groups on the virus are available to interact with negatively charged carboxyl groups on the carbon.

In most studies of protein or amino-acid adsorption on carbon, no effort has been made to control pH, because ampholytes tend to maintain pH values near their isolectric points. Tiselius (10) found that adsorption of mono-amino-dicarboxylic acids and di-amino-mono-carboxylic acids on carbon was strongly dependent on pH. Greatest adsorption occurred between pH 6.9 and 11.0. Adsorption of substances on activated carbon containing no amino or carboxyl groups indicate that different processes must be involved. For example, the adsorption rate of benzene-sulfonate steadily increased over the pH range 8.73 to 1.91 (11).

The interaction of carboxyl and amino groups is not the only mechanism leading to an optimum pH for adsorption rate. Configuration of the tail fibers on the phage is equally significant and also dependent on ionization of certain side groups. Virus tail fibers might be expected to adsorb on carbon by analogy with phage adsorption to host cells.

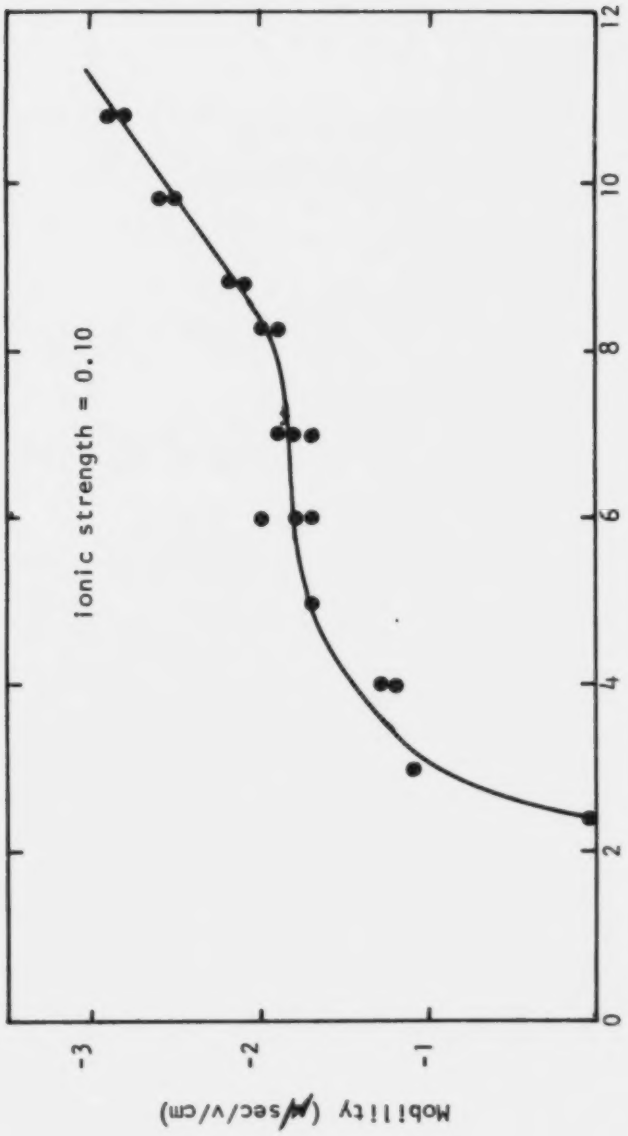

Figure 4. Variation of Mobility with pH for Untreated Carbon Particles

T-even bacteriophages have two distinct sedimentation rates in the ultracentrifuge. A rate of 1000 x 10^{-13} sec. occurs at pH 5.5 and goes through a transition to 700 x 10^{-13} sec. at pH 6.02 to 6.55 (12). The dual sedimentation rate also occurs when the ionic composition of the solution is changed (12). The reason for this dual behavior has been recently traced to the position of the tail fibers. At pH values from 6.0 to 9.5, tail fibers are extended as shown in Figure 1. At pH 5, however, they are not extended, but adsorb to the tail sheath (13). The pH, therefore, not only affects electrostatic interaction between phage and adsorbent, but also the position of tail fibers with respect to the tail sheath. The ionic strength effect indicates that tail fibers adsorb to activated carbon. Thus, viral tail fibers will not be extended for adsorption on carbon at pH's below 6.0 and above 9.5.

Determination of Active Groups on Carbon

The pH studies indicate that adsorption may involve amino and carboxyl groups. A large fraction of the acidic groups on carbon react with diazomethane and has been described as carboxyl and phenolic hydroxyl groups (14).

If carboxyl groups on carbon are the active units in virus adsorption, the adsorption capacity of carbon should be greatly reduced by esterification of the carboxyl group. Esters can be formed by the reaction of a carboxylic acid with an alcohol in the presence of a strong mineral acid.

The function of the acid catalyst is to protonate the carbonyl oxygen, thereby becoming more susceptible to attack by the alcohol molecule. Propylene oxide also was used for esterification. The epoxide ring of propylene oxide is cleaved under acid conditions. A carbonium ion intermediate is formed which causes ester formation with carboxyl groups. Carbon was treated with solutions of acid-alcohol, concentrated propylene oxide, and an acid solution of 80 percent propylene oxide.

Carbon suspensions were made in 0.1 N HCl in absolute methanol and in propylene oxide, and allowed to react for 2 days at 25°C. After reacting, the carbon was washed three times and suspended in deionized water to give 1000 mg/l. Washing involved repeated centrifugation, resuspension in deionized water, and shaking. Various reaction solutions of carbon and virus were then prepared. Optimum pH of 7.0 and ionic strength of 0.08 were obtained with phosphate buffer.

Adsorption of virus to treated carbon showed a marked reduction in carbon capacity (Fig. 5). The most pronounced effect occurred with the carbon treated with acid-alcohol. The change in virus concentration for 50 mg/l of untreated carbon was plotted in Fig. 5 for comparison.

Adsorption on acid-alcohol treated carbon reached equilibrium in 4 hours, adsorbing 2.0×10^7 virus particles per mg. Studies employing untreated carbon gave 1.5×10^9 virus particles per mg for an identical equilibrium concentration in solution. Thus, the carbon treated with acid-

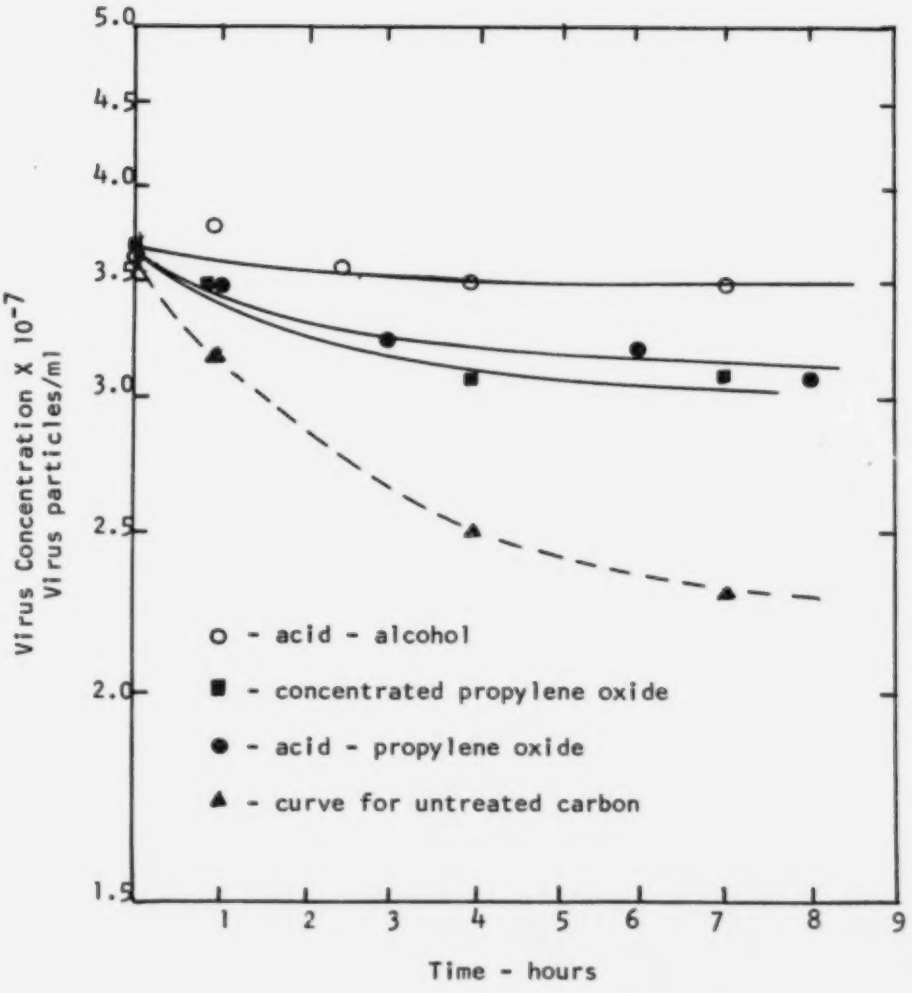

Figure 5. Adsorption of Bacteriophage T_4 on Carbon Teated with Carboxyl-Blocking Reagents

alcohol had its sites reduced by 99 percent. Treatment with propylene oxide reduced the available sites by 92 percent.

The use of acid as a catalyst with propylene oxide yielded no significant increase in site reduction over the pure propylene oxide treatment. Apparently, the acidic groups on carbon can supply the necessary protons to cleave the epoxide ring of propylene oxide.

In summary, these tests support the presence of carboxyl groups on activated carbon and demonstrate that they are the active groups in virus adsorption.

Effect of Ionic Strength on Adsorption

An experimental series was conducted varying ionic strength between 0.003 and 0.20. Control tests over the same range showed that virus inactivation was insignificant, except at extreme ionic strengths. Carbon concentrations were 250 mg/l, except that 240 mg/l was used in tests 3 and 4 (Table 2). The pH was buffered at 6.9. Two buffer systems (mono- and dipotassium phosphate and sodium bicarbonate) were used to check for differences in adsorption. Five percent CO_2 was continuously bubbled through the bicarbonate solution to maintain constant pH.

Adsorption rates at the various ionic strengths were determined from kinetic plots employing the reversible second-order equation, as illustrated in Fig. 6. Adsorption rates were determined from the slope of the fitted line in each kinetic plot, when plotted against ionic strength (Fig. 7), maximum rate occurred at 0.08.

Repulsive forces between colloids of like charge can be lowered by decreasing the distance of charge effectiveness, a function of the ionic strength of the solution. Interactions between like charges on activated carbon and virus are also weakened by an increase of ionic strength, due to formation of a diffuse double layer. Consequently, adsorption rate increases as ionic strength increases. Occurrence of a maximum and a decrease in adsorption rate at ionic strengths above 0.08, however, must result from another mechanism.

The most likely explanation appears to lie in the behavior of the viral tail fibers. Repulsion and interaction of tail fibers with the tail sheath have been discussed above in relation to pH effects. Tail fibers also change their configuration with ionic strength. Although no quantitative relation has been established between ionic strength and the degree of tail fiber extension, studies on sedimentation rates indicate that effects exist. Sharp and coauthors (15) found that the two sedimentation rates of 700×10^{-13} and 1000×10^{-13} sec, corresponding to extended and retracted tail fibers, could be obtained by changing the ion composition as well as pH of the solution. Kellenberger and coauthors (16) noted that three tail fibers of bacteriophage T_4 are extended at an ionic strength of 0.1. In deionized water, however, more fibers were extended. As discussed above, like charges exert their greatest repulsive forces at low ionic strengths.

TABLE 2

TEST SOLUTIONS OF VARIOUS IONIC STRENGTHS
FOR STUDYING VIRUS ADSORPTION ON CARBON

Test No.	Ionic Strength			Virus concentration per ml	Buffer System
	Buffer	NaCl	Total		
1	0.005	0.002	0.007	4.8×10^8	bicarbonate
2	Zero	0.003	0.003	4.7×10^8	none
3	0.001	0.003	0.004	7.3×10^8	phosphate
4	0.087	0.003	0.090	6.0×10^8	phosphate
5	0.036	0.004	0.040	4.0×10^8	phosphate
6	0.014	0.006	0.020	4.2×10^8	phosphate
7	0.076	0.044	0.120	4.9×10^8	phosphate
8	0.071	0.129	0.200	4.2×10^8	phosphate
9	0.007	0.003	0.010	4.0×10^8	phosphate
10	0.012	0.003	0.015	7.2×10^8	phosphate
11	0.014	0.006	0.020	1.1×10^8	phosphate
12	0.071	0.129	0.200	1.1×10^8	phosphate
13	0.080	0.020	0.100	4.8×10^8	phosphate
14	0.080	0.020	0.100	1.0×10^8	phosphate
15	0.080	0.000	0.080	1.0×10^8	phosphate
16	0.080	0.000	0.080	1.1×10^8	phosphate
17	0.080	0.020	0.100	1.2×10^8	phosphate
18	0.080	0.000	0.080	1.5×10^8	phosphate
19	0.080	0.000	0.080	4.7×10^8	phosphate
20	0.063	0.000	0.063	4.2×10^8	phosphate
21	0.063	0.000	0.063	1.5×10^8	phosphate
22	0.063	0.000	0.063	1.1×10^8	phosphate

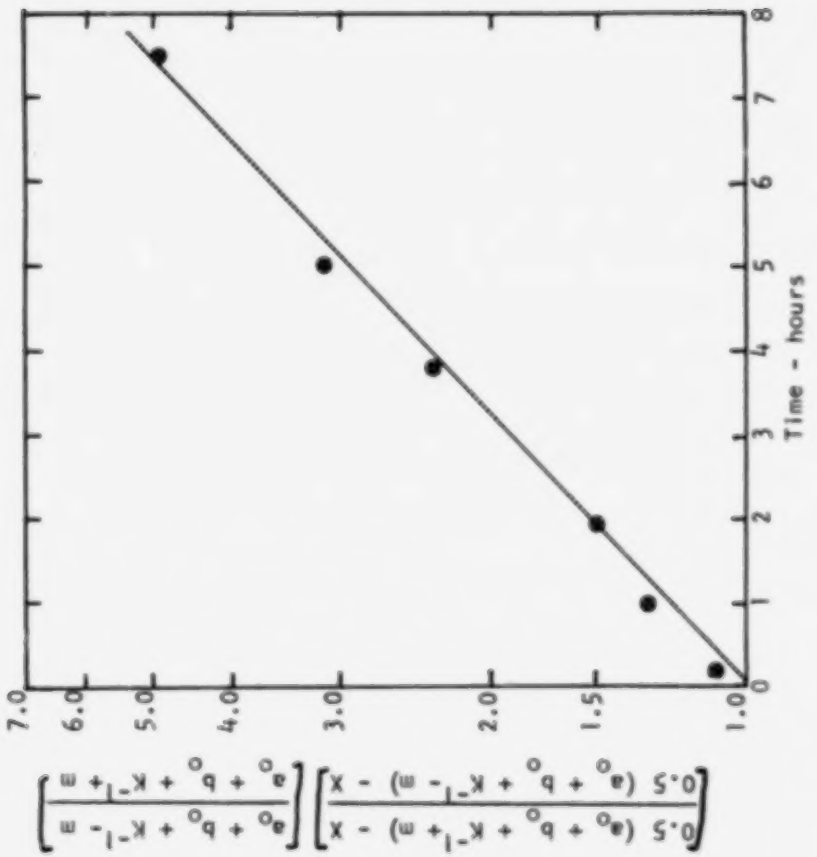

Figure 6. Reversible second-order kinetic plot of adsorption of T_4 phage on carbon at ionic strength 0.063

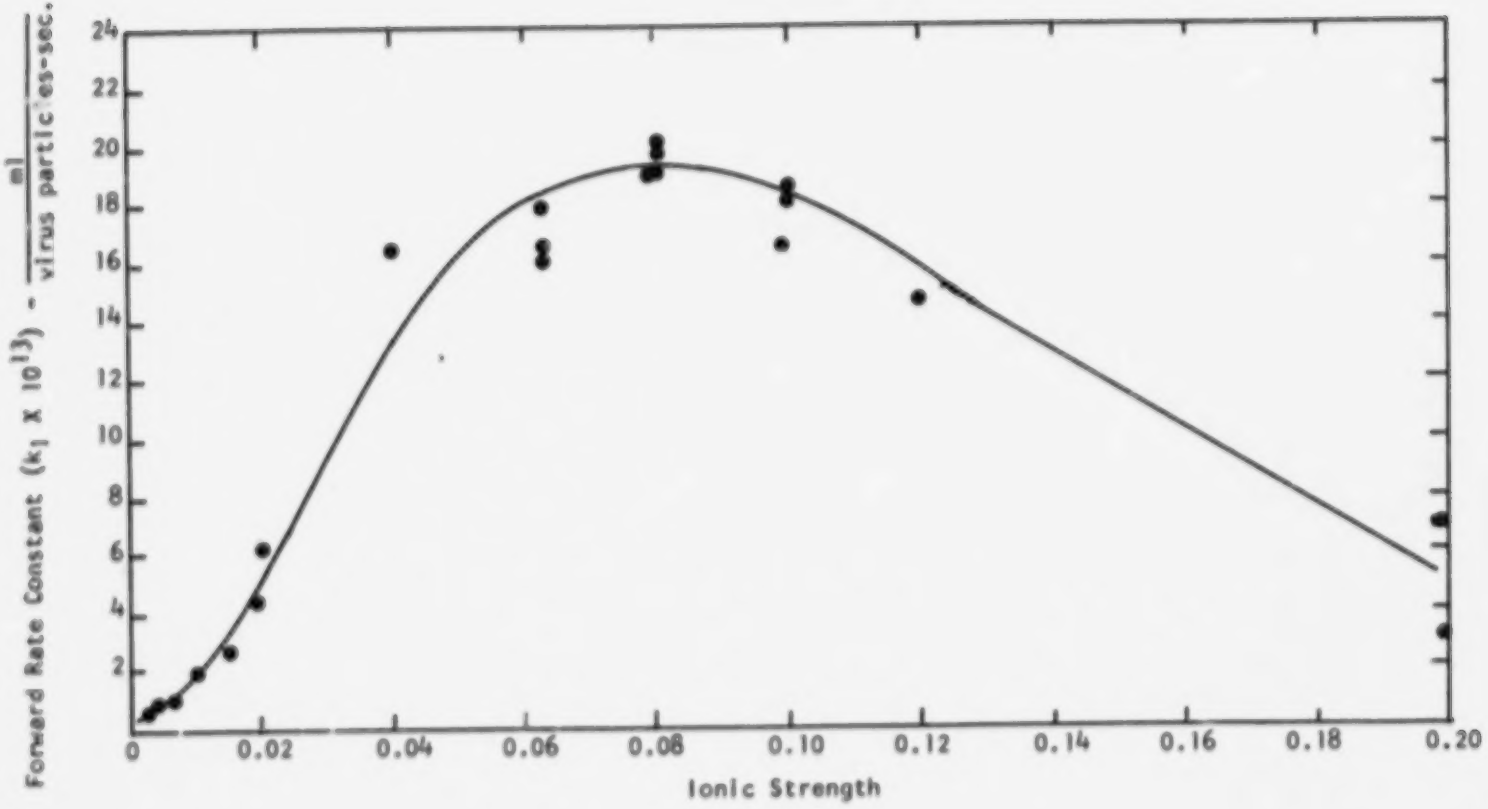

Figure 7. Forward Rate Constant (k_1) vs. Ionic Strength for Adsorption of T_4 Phage to Carbon

This condition causes the fibers to be repelled from the tail sheath and exposes their sites for adsorption on the adsorbent. As ionic strength is increased, the interaction of the like charges is weakened, and this allows the fibers to adsorb on the tail sheath. Their sites, therefore, are not exposed for attachment to the adsorbent.

Effect of Ionic Strength on Equilibrium

Further confirmation of the mechanism proposed above can be sought from the behavior of the virus-carbon system at equilibrium. Equilibrium conditions should not varywith ionic strengths below the optimum, but higher than optimum ionic strengths should shift the equilibrium condition toward a decrease in adsorbed viruses.

General equilibrium conditions at optimum pH and ionic strength follow the Langmuir isotherm (4) (Fig. 8).

Influences on equilibrium were sought from four adsorption tests at a relatively low ionic strength (0.02) and three at a high ionic strength (0.20). The tests were made with T_4 phage and a phosphate buffer system at pH 6.9. Equilibrium was achieved after 22 to 25 hours.

After 22 hours of adsorption at ionic strength 0.02, the first-order rate of the reaction was approximately 0.02/hr, which was equivalent to the natural inactivation rate of the virus at the same ionic strength. The four tests at ionic strength 0.02 were corrected for inactivation and compared with existing equilibrium values obtained at the optimum ionic strength of 0.08 (Fig. 8). All points

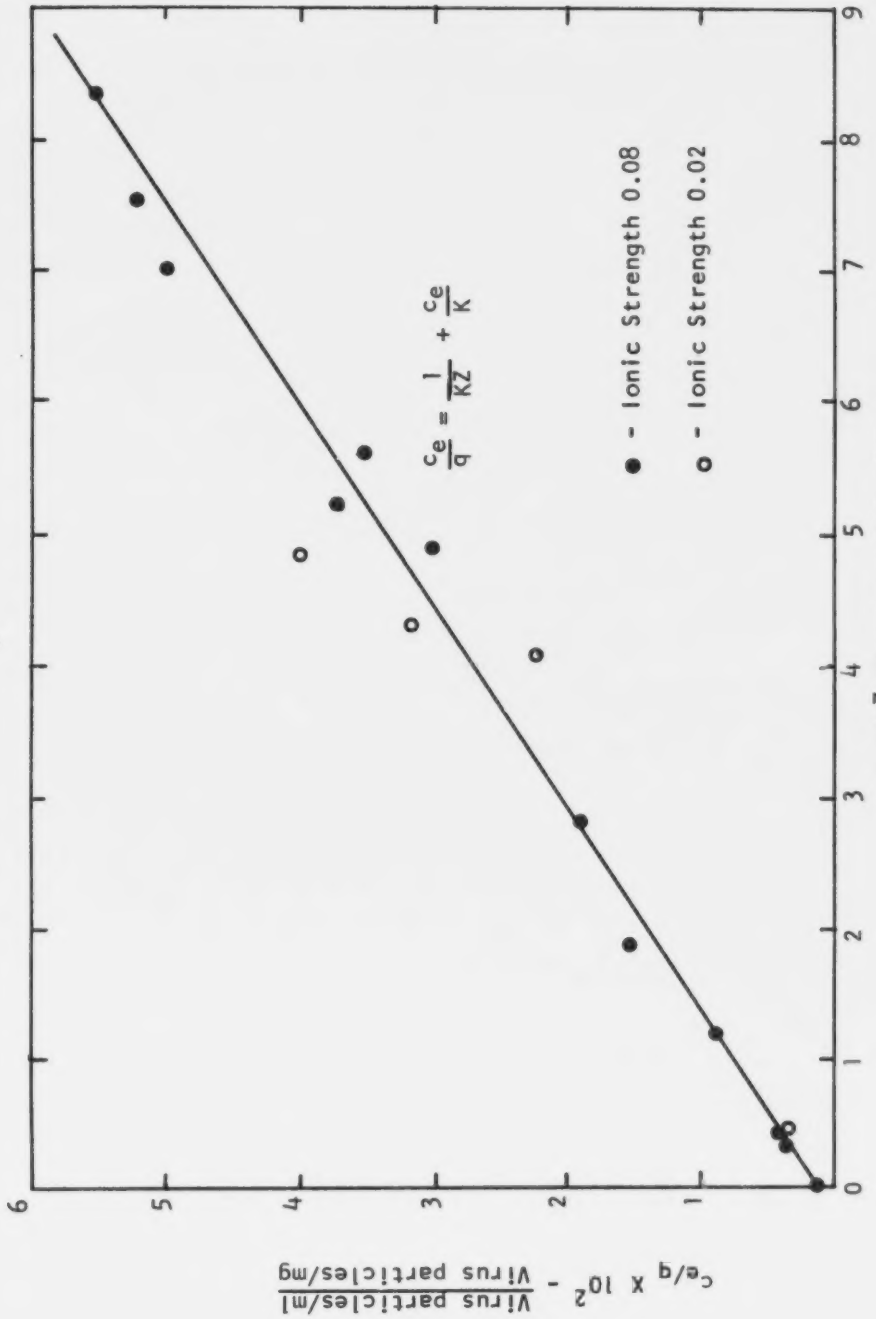
$\frac{c_e}{q} = \frac{1}{KZ} + \frac{c_e}{K}$
● - Ionic Strength 0.08
o - Ionic Strength 0.02
c_e X 10^{-7} Virus particles/ml
c_e/q X 10^2 - $\frac{\text{Virus particles/ml}}{\text{Virus particles/mg}}$

Figure 8. Langmuir Plot for Adsorption of T_4 Phage on Activated Carbon by Least Squares Analysis

corresponded reasonably well with previous data. It was concluded that low ionic strengths did not change equilibrium conditions significantly.

A significant difference was found in the time required to reach equilibrium at the low ionic strengths. Apparently, the number of sites on the carbon and virus was not changed significantly by the low ionic strength, but the ability of the virus to reach these sites was lowered. This finding agrees with the described mechanism.

Three equilibrium tests were made at an ionic strength of 0.20 and pH 6.9. The Langmuir plot at this ionic strength illustrates a significant change in the equilibrium conditions (Fig. 9). The plot in Fig. 9 gave a value of 4.5×10^8 sites per milligram of carbon, compared to 1.6×10^9 sites/mg at at ionic strength of 0.08 (Fig. 8). Adsorption data at ionic strengths of 0.20 yielded a value for the equilibrium constant of 1×10^{-7} ml/virus particle, while at 0.08 a value of 4×10^{-7} ml/virus particle was obtained, suggesting that carbon capacity is reduced at higher ionic strengths. The results, however, can be explained by presuming that tail fibers are the agents adsorbing to carbon. In this case, the capacity of the carbon for viruses is not altered, as indicated by the Langmuir equation. Instead, the effect results from inability of a large portion of the virus population to adsorb because of interaction between the tail fibers and the tail sheath. The effective concentration of virus (those able to adsorb) would

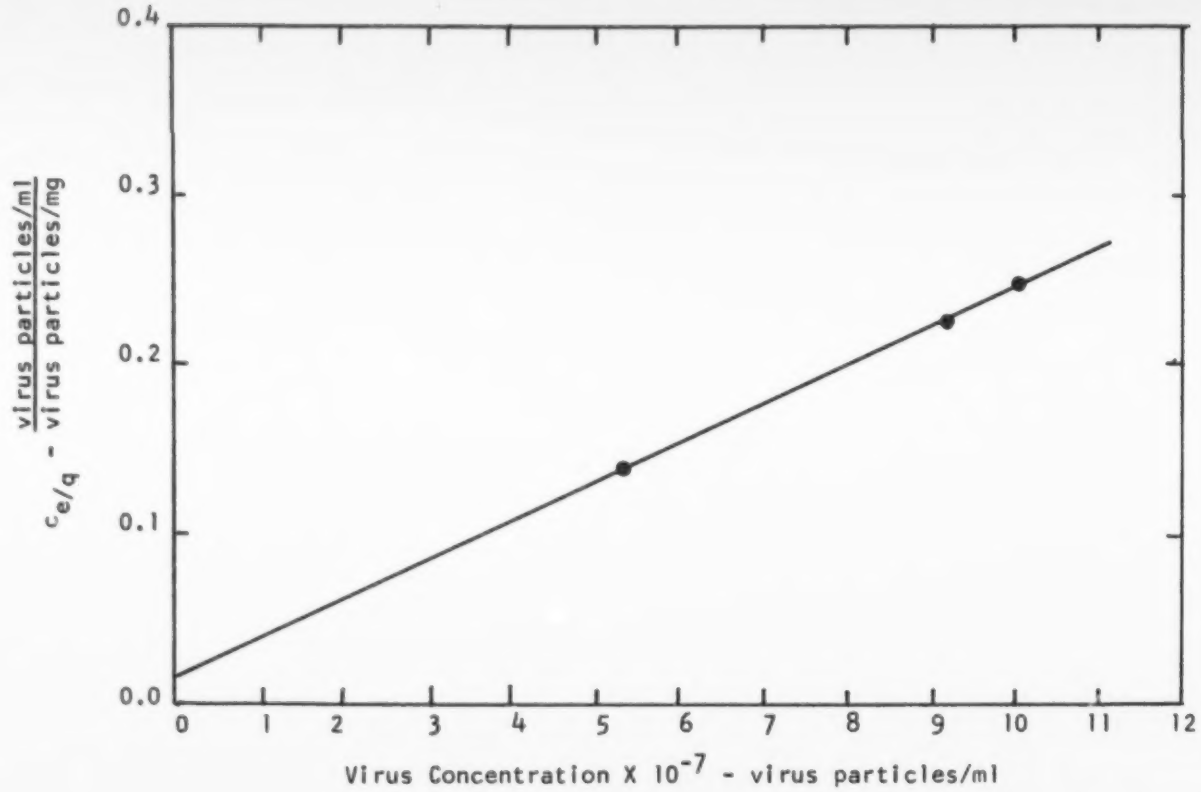

Figure 9. Langmuir Plot for Equilibrium in a Solution of 0.20 Ionic Strength and pH 6.9 by Least Squares Analysis

be much less than that given by the assay at equilibrium

In summary, two mechanisms interact to produce the observed effects of ionic strength. At ionic strengths less than optimum, the adsorption rate increases with increasing ionic strength. This is caused by masking of like charges between virus and carbon particles, allowing a greater collision frequency. At ionic strengths greater than the optimum, the adsorption rate decreases with increasing ionic strength. This may result from a change in the configuration of viral tail fibers. At low ionic strengths the fibers are extended. This position favors adsorption of viruses to carbon. At high ionic strengths like charges are masked on the tail fibers and tail sheath, causing fiber withdrawal and adsorption to the tail sheath. This inactivates viruses for adsorption on the carbon.

Conclusions

Sites on activated carbon that adsorb bacteriophage T_4 are probably a carboxyl group or lactone. Adsorption on carbon can be completely blocked by esterifying these groups.

It is proposed that amino groups on the virus adsorb to carboxyl groups on the carbon by electrostatic attraction. The pH range of strong adsorption rules out participation by ionized forms of sulfhydryl, guanidino, and phenolic groups in the electrostatic binding. Ionized imidazolyl groups are probably too few to be significant.

As pH decreases from the optimum of 7.0, adsorption rate decreases, probably as a result of viral tail fibers

being attached to the tail sheath, making them unavailable for attachment to carbon sites.

At pH values higher than optimum, the tail fibers of bacteriophage T_4 are extended. The observed decrease in adsorption rate presumably resulted from an increase of negative charge on the virus particles and carbon surface, causing greater repulsive forces between viruses and carbon particles. The collision frequency, therefore, was reduced.

Electrostatic binding of virus and carbon, and designation of viral tail fibers as the adsorbing units, received support from the effect of ionic strength on adsorption. With increasing ionic strength, adsorption is aided as like charges on the virus and carbon particles are masked; but, at the same time, repulsive forces between the viral tail fibers and tail sheath are reduced. With increasing ionic strength, more and more tail fibers adsorb on the tail sheath. Although high ionic strengths cause a maximum collision frequency between virus and carbon particles, the adsorbing tail fibers become less available. These mechanisms are supported by equilibrium studies at high and low ionic strengths.

References

1. Pyl, G., Adsorptionsversuche with Maul- and Klauenseuchevirus in Puffer lösungen. Zentralblatt Für Bakteriologie Parasitenkunde und Infektionskrankheiten. 121:10 (1931).

2. Poppe, K., and Busch, G., Physikalische und chemische Untersuchungen am Virus der Maul-und Klauenseuche I. Isoelektrischer Punkt und Adsorption. Zeitschriff fur Immunitätsforschung und experimentelle Therapie. 68:510 (1930).

3. Clarke, N. A., and Chang, S. L., Enteric Viruses in Water. Jour. AWWA. 51: 1299 (1959).

4. Cookson, J. T., Jr., and North, W. J., Adsorption of Viruses on Activated Carbon: Equilibria and Kinetics of the Attachment of Escherichia coli Bacteriophage T_4 on Activated Carbon. Environmental Science and Technology. 1:46 (1967).

5. Cookson, J. T., Jr., Adosrption of Viruses on Activated Carbon: Adsorption of Escherichia coli Bacteriophage T_4 on Activated Carbon as Diffusion-Limited Process. Environmental Science and Technology. 1:157 (1967).

6. Questionnaire and Correspondence from West Virginia Pulp and Paper Company (1964).

7. Juhola, A. J., and Wiig, E. O., Pore Structure in Activated Charcoal II. Determination of Micro Pore Size Distribution. Amer. Chem. Soc. 71:2078 (1949).

8. Stent, G, S., Molecular Biology of Bacterial Viruses. W. H. Freeman and Company, San Francisco, California (1963).

9. Black, A. P., and Smith, A. L., Determination of the Mobility of Colloidal Particles by Microelectrophoresis, Journal American Water Works Association, 54:926 (1962).

10. Tiselius, A., Adsorption analysis of amino acids and peptides. Arkiv För Kemi, Mineralogi Och Geologi. 15B: No. 6, 1 (1941).

11. Morris, J. C., and Weber, W. J., Adsorption of Biochemically Resistant Materials from Solution. Environmental Health Series AWTR-9, U. S. Department of Health, Education, and Welfare (May, 1964).

12. Bendet, I. J., Swaby, L. G., and Lauffer, M. A., Dual Sedimentation of T_2 Bacteriophage of Escherichia coli. Biochemica et Biophysica Acta. 25:252 (1957).

13. Lauffer, M. A., and Bendet, I. J., Comments on Biophysical properties of bacteriophage T_2. Biochimica et Biophysica Acta. 55:211 (1962).

14. Boehm, H. P., Chemical Identification of Surface Groups, Advances in Catalysis, Vol. 16, edited by D. D. Eley, H. Pines, and P. B. Weisz, Academic Press, New York, N. Y. 1966.

15. Sharp, D. G., Hook, A. E., Taylor, A. R., Beard, D., and Beard, J. W., Sedimentation Characters and pH Stability of the T_2 Bacteriophage of Escherichia coli. Jour. Biol. Chem. 165:259 (1946).

16. Kellenberger, E., Bolle, A., Boy de la Tour, E., Epstein, R. H., Franklin, N. C., Jerne, N. K., Reale-scafati, A., and Séchaud, J., Functions and Properties Related to the Tail Fibers of Bacteriophage T_4. Virology. 26:419 (1965).

Acknowledgments

Part of the research presented in this section was conducted at the California Institute of Technology and supported by U. S. P. H. Training Grant (5T 1 ES - 04).

PART III

APPLICATION OF MASS TRANSFER THEORY TO FILTRATION

Filtration has been extensively investigated, but much of the work concerning filtration was primarily empirical. None of the proposed empirical equations correlate all variables, making it impossible to evaluate the effects of variables on filtration efficiency. In recent years, innovations have altered the old concepts of filtration and theoretical advances have given impetus to the formulation of filtration theories.

Filtration efficiency depends on physical and chemical parameters which can be described by two steps, a particle transport and an attachment step. Particle attachment is brought about by colloid-chemical forces controlled by the surface properties of the respective materials and van der Waals forces (Ives and Gregory, 1966). In filtration, these forces result from interactions between the surface of the filter media and the suspended-aqueous phase particles. Chemical effects in filtration are supported by correlation between electrophoretic mobility of suspended particles and their removal (Jorden 1963). Removal of clay colloids and bacteria by sand filters appears to depend on clay micelle orientation, diffusion, van der Waals forces, and electrokinetic forces (Edwards and Monke, 1967). It will be the purpose of this paper to consider the physical process of filtration, that is the particle transport step.

Physical Filtration Theories

Physical filtration mechanisms include straining, sedimentation, inertial impingment, and diffusion. An excellent discussion of these has been presented by O'Melia and Crapps (1964). Traditional concepts of rapid sand filtration have

assumed that suspended-particle removal is accomplished primarily by straining, sedimentation, or both, and have been generally described by various empirical equations. Ives and Shalji (1965) have recently developed a theoretical representation of physical filtration based on gravitational forces. They propose a model by evaluating the relationships between filter efficiency and the variables of media size, flow velocity, and water viscosity. Although the theory of Ives and Sholji is probably the most comprehensive in describing physical filtration, it is limited to particle sizes that are mainly influenced by gravitational forces.

The first attempts to explain filtration of small particles have originated from aerosol filtration data. Friedlander (1958) correlated data on aerosol filtration by fibrous filters operated at low Reynolds numbers to parameters based on diffusion and direct interception. O'Melia and Stumm (1967), using Friedlander's model, illustrated that diffusion and not direct interception was the major contributor to contact efficiency of suspended particles of 3 microns or smaller. For particles of 0.3 microns in size, diffusion almost solely governed contact efficiency. Traditionally, little importance has been given to diffusion models for water filtration, but studies presented by Robeck (1963) indicate that the great majority of the suspended particles in the influent to rapid sand filters are smaller than 3 microns in diameter. These studies indicate that diffusion is important, and the transport step in filtration may be limited by a diffusion process. A better model

for filtration would then be obtained from consideration of diffusion in a flowing fluid.

This study examines the removal of viruses through packed beds and evaluates the theory of mass transfer, based on the thin boundary layer solution of the diffusion equation, for water filtration systems. The removal of bacteriophage T_4 by activated carbon beds is examined under varying conditions of bed length, grain diameter, bed porosity, and flow rate. Virus removal and filtration variables are interpreted by mass transfer theory. Although this study is devoted to virus removal in activated carbon beds, it should be emphasized that the model will apply to any colloid being removed in porous beds where diffusion is the limiting step. This study has many ramifications, since it will apply to the removal of color and other organics by filtration units and adsorption beds.

Viruses are transmitted by water and the need for further knowledge on virus removal has been emphasized as a prerequisite to water quality control. Viruses are also very uniform in size and shape and can be assayed with a high degree of accuracy. One assays individual virus particles and not molar concentration.

Activated carbon was used as the bed medium since it has high adsorptive capacity for many colloids found in water. Virus adsorption on activated carbon has been described as a diffusion limited process, thus making it an ideal system for

studying particle transport in filtration and the adaptation of a mass transfer model to water filtration.

Mass Transfer Theory

The goal of any filtration theory is to predict the effect of variables on removal efficiency. Particle removal in a filter can be related to a transfer coefficient, k. In a fixed bed, the rate of transfer between inlet and outlet conditions of the bed is described by the equation

$$G(C_1 - C_2) = k A_m \Delta C_{lm} V \qquad (1)$$

In Equation 1, G is the flow rate, A_m the surface area per unit volume of packing, V the bed volume, ΔC_{lm} the log mean concentration, and C_1, C_2 the inlet and outlet concentrations. From the transfer coefficient, bed characteristics and flow rate, Equation 1 can be used to predict filtration efficiency. Direct application of Equation 1, however, depends on the ability to calculate k from the theory of diffusional exchange between flowing fluids and surfaces.

Mass transfer coefficient is often expressed in the dimensionless Sherwood number, Sh. Mass transfer models can be expressed in terms of the Sherwood number and the dimensionless Péclet number, Pe. The Péclet number is a measure of the ratio of transport by convective forces to transport by molecular diffusion. The theory of heat transfer in a flowing fluid has been extensively investigated and can be directly applied to mass transfer. Theoretical approaches have used the boundary-layer theory and the von Karmon integral relation. This approach involves the assumption that a concentration boundary

layer exists. This boundary layer is a limited region of flow around the surface of the filter medium and is affected by the presence of this surface. Resistance to mass transfer is assumed to reside in this boundary layer. The driving force for mass transfer is the concentration difference across the boundary layer. The concentration of colloid or solute adjacent to the bed solid is the equilibrium concentration for adsorption systems or the saturation concentration for dissolution of solute. At the edge of the boundary layer, the concentration reaches the main-stream value. If a concentration distribution is assumed to exist across this boundary layer, and the concentration boundary layer coincides with the velocity boundary layer, then the mass transfer rate can be calculated by use of the known velocity distribution and a mass balance. Various alterations to the mass transfer problem have been developed.

Pfeffer and Happel (1964) extended mass transfer theory to include multiparticle systems. Their model is developed on the basis that two concentric spheres will describe a typical cell in a random assemblage consisting of many cells, each of which contains a particle surrounded by a fluid envelope. Each cell is assumed to contain a spherical fluid envelope whose relative volume to the particle volume is the same as that of the whole assemblage. The entire disturbance due to each particle is confined to the cell of fluid with which it is associated. Thus, the concentration of the forward moving fluid is that of the cell boundary.

From Pfeffer and Happel's (1964) derivation, the Sherwood number (Sh) is a function of the Péclet number (Pe) and void

fraction, and at high Péclet numbers (Pe > 70), the Sherwood number can be expressed as a simple exponential function of the Péclet number:

$$Sh = Be\ Pe^{1/3} \tag{2}$$

Be is given by:

$$Be = 1.26\left[\frac{1 - r^5}{W}\right] \tag{3}$$

where

$$W = 2 - 3r + 3r^5 - 2r^6 \tag{4}$$

and the fractional void volume, ϵ , of a multiparticle system is directly related to r , the geometry of the free surface model by the expression:

$$\epsilon = 1 - r^3 \tag{5}$$

For a single particle in a flowing fluid, $\epsilon = 1$, Equation 2 reduces to

$$Sh = 0.997\ Pe^{1/3} \tag{6}$$

Mass transfer data for packed beds are usually correlated to the dimensionless j or Colburn factor, which takes into account system characteristics and is defined by

$$j = \frac{Sh}{Re\ Sc^{1/3}} = \frac{k}{u}\left(\frac{\nu}{D}\right)^{-1/3} \tag{7}$$

and since

$$Pe = Re\ Sc \tag{8}$$

therefore

$$j = Be\ Re^{-2/3} \tag{9}$$

Thus, the Colburn factor is a function of the Reynolds number, Re, and a constant dependent on void fraction. This equation can be rewritten as follows:

$$j = 1.26 \left[\frac{1-(1-\epsilon)^{5/3}}{W}\right]^{1/3} Re^{-2/3} \qquad (10)$$

In order to compare data taken at different void volumes, Equation 10 is written in terms of a pseudo-Reynolds number, N_{Re}, which depends on the void fraction.

$$j = 1.26 \left\{\left[\frac{1-(1-\epsilon)^{5/3}}{W}\right]^{-1/2} Re\right\}^{-2/3} \qquad (11)$$

$$j = 1.26\, N_{Re}^{-2/3} \qquad (12)$$

The mass transfer coefficient, k, can be determined from Equations 7 and 9 and used in Equation 1 to predict filtration efficiency. This model was evaluated by correlation of experimental values of j and Reynolds number to the theoretical relationship expressed by Equation 9.

Experimental Procedure

Filtration columns of various diameters were made from plexiglass tubing (Figure 1). Columns were from 4.2 cm. to 25.2 cm. in length. The ends of each column were equipped with tubing connectors for the flow meter, pump, and manometer. A rubber or cork gasket and a copper screen (100 mesh) for supporting the bed media were placed between each flange. The column was packed by repeated addition of small amounts of activated carbon and tapping in order to obtain the greatest compaction. A peristaltic pump, consisting of a combination of masterflux pump heads and a servodyne power drive system

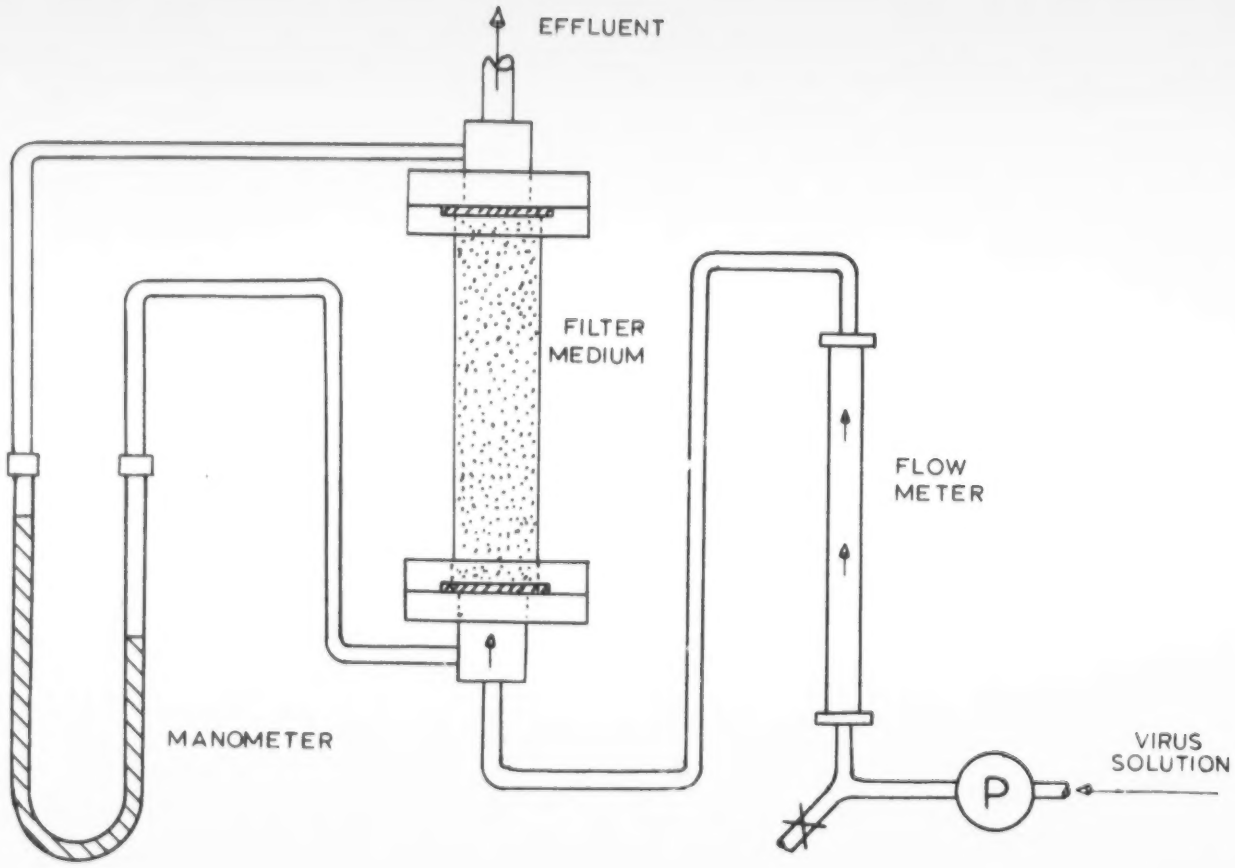

Figure 1. Filtration apparatus

provided excellent control of the flow rate. Flow rate was monitored by rotameters. An 18" U-Type manometer was used to determine pressure drop in the packed beds during filtration.

In order to prevent the adsorption of viruses to glassware, positive charges were removed by washing in an alkali-detergent mixture. After washing, glassware was rinsed in tap water, rinsed with distilled water, and then sterilized in a hot air oven at 200°C. for one hour. The activated carbon was sterilized by autoclaving. Pumping equipment and accessories were sterilized before each test run with a mixture of penicillin (100 units/ml.), and streptomycin (0.2 mg./l.). After a contact time of two hours, the pumping equipment was rinsed by passing sterilized distilled water through the system.

Application of mass transfer theory requires knowledge of the media particle size and the void fraction of the packed bed. Particle sizes were initially determined by microscopic examination and void fractions by immersion of the activated carbon bed in water. A Porton's Graticule was used to size the granular carbon microscopically. Three different mesh sizes of carbon were sized and used in the filtration studies (Table 1).

The determination of void fraction by water immersion was found to be unrealistic for activated carbon beds. This discrepancy was revealed by pressure losses monitored during each filter run. Water immersion gave high void fractions, a result of the carbon's ability to sorb water in inner pores and other dead-end areas that do not constitute porosity

related to the flow regime of the packed bed. If each particle is considered to be surrounded by an impervious envelope, the void volume needed is the space between the envelope particles; and the area of the enveloping surface per unit enveloped volume is known as the specific surface.

The effective void fraction (ϵ) of the activated carbon beds was calculated from experimentally determined values for the bulk density (ρ_B) of the packed column and the particle density (ρ) of the activated carbon.

$$\epsilon = 1 - \rho_B/\rho \tag{13}$$

The particle density of crushed porous materials can be determined from gas-flow rate, pressure drop and bulk density measurements in packed columns. This method was first outlined and discussed by Ergun (1951). The method is based upon the determination of the values (a) and (b) of the pressure drop Equation (14) at different bulk densities to which a given porous material may be packed:

$$\frac{\Delta P}{Lu} g = a + bU \tag{14}$$

where

$$a = 150 \frac{(1-\epsilon)^2}{\epsilon^3} \frac{\mu}{D_m^2} \tag{15}$$

$$b = 1.75 \frac{1-\epsilon}{\epsilon^3} \frac{1}{D_m} \tag{16}$$

The intercept (a) and slope (b) can be obtained by plotting $\frac{\Delta P}{Lu} g$ versus U. The void fraction, ϵ , and the effective diameter, D_m, are the only variables that (a) and (b) are dependent upon. Since the effective diameter is constant for a

particle of a given size, the effect upon changing the intercept or the slope will make it possible to determine the void fraction.

A total of 118 flow rate-pressure drop measurements were made at ten different bulk densities. Typical plots are given in Figure 2 from which values of (a) and (b) were determined by the method of least squares. An average particle density of 0.202 gm. per cm.^{3} was obtained for the 20/30 size carbon. The range of values was 0.196 to 0.209 gm. per cm.^{3}. The 550 and 248-micron carbons were assumed to have the same particle density of 0.202 gm. per cm.^{3}. The average pore size of activated carbon is about 20 microns. The 550 and 248-micron particles should have about the same pore volume per weight as the 992-micron carbon, and, consequently, nearly the same particle density. Particle properties determined by the pressure drop technique confirmed those obtained by microscopic techniques (Table 1). From the particle and bulk densities, the void fraction was calculated for each mass transfer test.

The procedures of Cookson and North (1967) were used for assaying and preparing bacteriophage T_4 stock solutions and Escherichia coli B host cells. The filtration solution of virus was buffered at pH 7.0 with mono-dipotassium phosphate of ionic strength of 0.10. This pH and ionic strength provide the optimum condition for virus attachment to carbon. For each mass transfer test, samples were collected (1) from the buffered virus solution, (2) at the inlet of the filter column to determine any virus loss through the pump, and (3) at the outlet of

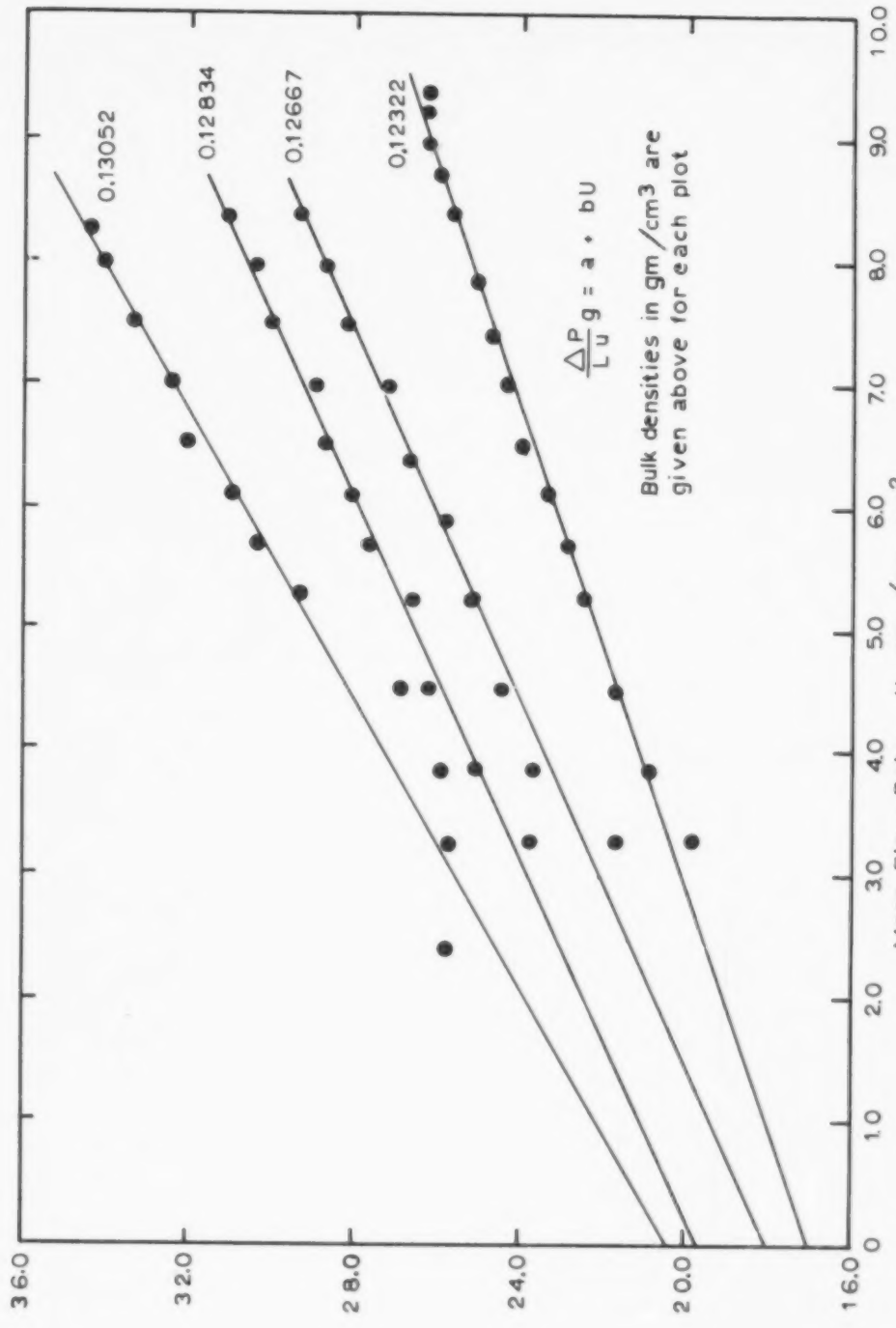

Figure 2. Typical plots of pressure-drop equation at different bulk densities

TABLE 1

PHYSICAL CHARACTERISTICS OF ACTIVATED CARBON

Mesh[d] Size	Number of Particles Sized	Mean Effective Diameter (microns) Dm	Specific Surface ($cm.^2$ per $cm.^3$) Sv	Total Surface[c] Area ($cm.^2$ per gm.)
20/30	1913[a]	982[a]	60.10[a]	397[a]
30/40	893[a]	550[a]	109.3[a]	779[a]
70/80	1918[a]	248[a]	241.6[a]	1715[a]
20/30	--	992[b]	60.50[b]	357[b]

[a] Determine by microscopic examination

[b] Determine by pressure drop studies

[d] Particles passed a U. S. standard sieve No. 20 but were retained on No. 30, etc.

[c] Determine by microscopic counting of number of particles per gram

Note: $D_m = 6/Sv$ for spherical particles

the filter bed. Different flow rates were examined for each column by starting with the highest flow initially and then progressively decreasing.

Virus Removal Through Packed Beds

Since the packed bed removes a greater portion of the viruses upon initial contact with the bed, an average concentration value from the influent and effluent does not adequately describe the virus concentration of the flow through the bed. Consequently, a log-mean virus concentration value is used.

$$\text{log-mean concentration, } \Delta C_{lm} = \frac{(C_1 - C^*)-(C_2 - C^*)}{\ln \frac{(C_1 - C^*)}{(C_2 - C^*)}} \quad (17)$$

The equilibrium concentration, C^*, at the surface of the carbon media is found by applying the Langmuir Isotherm, according to Cookson and North (1967).

In this study, tests were made under conditions where C^* was small (200 viruses/cm.^{3}) compared to inlet and outlet virus concentrations of about 1×10^6 and 4×10^4 viruses per cm.^{3}, respectively. In other words, the filter bed was operated well below its saturation point. Therefore, the equilibrium concentration term has been neglected when determining the log-mean virus concentration.

Experimental Results

Virus removal was monitored through nine carbon beds, each bed being subjected to different flow rates. Physical characteristics were not identical for any of the nine columns

(Table 2). Parameters for mass transfer have been calculated for each column tested, incorporating the varying conditions of media size, column length, column area, void fraction, and flow rate (Table 3). In Mass Transfer Test 4, which used the 248-micron carbon, all of the virus particles were removed as none were detected in the effluent samples. The assay procedure requires a minimum of 2000 viruses per $cm.^3$ for detection. For comparison with results of other tests, 1 virus per $cm.^3$ was assumed to have passed through the column (Table 3).

As discussed above, the theoretical correlation of Colburn factor to Reynolds number predicts an exponent of -2/3 for systems with a Péclet number greater than 70. All Péclet numbers in these tests were greater than 1000. The Reynolds number exponent varied from -0.50 to -0.66 (Table 4).

The experimental exponent may differ from the theoretical because of deficiencies in the basic mass transfer model. Virus desorption will occur when the bed is near saturation. Application of mass transfer theory (Equation 9) requires knowledge of the equilibrium concentration. That is, the virus concentration in solution at which the rate of virus adsorption equals that of desorption. A simplified equilibrium concentration, based on the total capacity of the carbon bed, was calculated from equilibrium studies of Cookson and North (1967). The maximum equilibrium concentration for each test was under 300 viruses per $cm.^3$, which is negligible compared to the virus concentration in the bulk flow. Little virus desorption is expected to occur from the column, but desorption and readsorption will occur

TABLE 2

COLUMN AND BED CHARACTERISTICS

Test No.	Height cm	Area cm^2	Calculated Void Fraction	Particle Diameter cmx10^2	A_m cm^2/cm^3
#1	8.60	0.375	0.345	9.87	50.0
#2	8.59	0.405	0.296	9.87	53.4
#3	4.20	0.385	0.236	2.48	264.0
#4	7.50	0.664	0.277	2.48	253.0
#5	12.40	1.330	0.330	9.87	50.8
#6	25.20	2.010	0.315	9.87	52.2
#7	25.20	2.010	0.299	9.87	53.0
#8	25.20	2.010	0.278	9.87	54.9
#9	12.40	1.330	0.413	5.50	91.6

TABLE 3

FILTRATION DATA

Test No.	Flow Rate G cm^3/sec	$\frac{\Delta P}{Lu} \times 10^{-3}$ $\frac{dyne\text{-}sec}{cm^4}$	Inlet Virus Conc, virus/$cm.^3$	Outlet Virus Conc, virus/$cm.^3$	Transfer Coef., $(k \times 10^4)$ cm/sec	Re	j	$N_{Re} \times 10^1$	$j\epsilon$
#1	0.3020	not	1.4×10^8	1.1×10^8	4.66	7.92	1.44	15.2	0.50
	0.1685	measured	1.4×10^8	1.0×10^8	3.52	4.43	1.95	8.5	0.67
#2	0.1718	not	1.5×10^6	1.0×10^6	3.76	4.36	2.21	7.04	0.65
	0.1533	measured	1.5×10^6	9.6×10^5	3.67	3.74	2.42	6.04	0.72
#3	0.446	61.9	9.1×10^5	2.7×10^5	12.50	2.87	2.70	3.57	0.64
	0.252	61.2	9.1×10^5	2.0×10^5	8.89	1.62	3.39	2.02	0.80
	0.167	53.4	9.1×10^5	1.1×10^5	8.19	1.08	4.71	1.35	1.11
#4	0.076	133.0	9.3×10^5	0					
	0.056	117.0	9.3×10^5	0					
	0.042	12 .0	9.3×10^5	0	4.52	0.158	17.85	0.24	4.95
#5	0.636	63.4	1.1×10^6	6.8×10^5	3.54	4.71	1.87	8.57	0.62
	0.550	62.2	1.1×10^6	6.4×10^5	3.46	4.09	2.09	7.44	0.68
	0.467	61.9	1.1×10^6	6.0×10^5	3.29	3.47	2.36	6.32	0.78
	0.380	61.8	1.1×10^6	5.7×10^5	2.90	2.82	2.53	5.13	0.84
	0.292	64.5	1.1×10^6	5.3×10^5	2.47	2.16	2.81	3.93	0.93
	0.210	62.2	1.1×10^6	4.8×10^5	2.01	1.56	3.18	2.84	1.05
	0.122	54.9	1.1×10^6	3.0×10^5	1.84	0.91	5.01	1.65	1.66

$$S_c = \frac{\nu}{D} = 1.25 \times 10^5$$

TABLE 3 (Cont'd)

Test No.	Flow Rate G cm3/sec	$\frac{\Delta P}{Lu}$ x10^{-3} $\frac{\text{dyne-sec}}{cm^4}$	Inlet Virus Conc, virus/cm.^{3} x 10^{-6}	Outlet Virus Conc, virus/cm.^{3} x 10^{-5}	Transfer Coef., (kx10^4) cm/sec	Re	J	N_{Re}x10^1	j_ϵ
#6	4.370	5.14	1.0	6.7	6.60	21.45	0.76	36.9	0.24
	3.770	5.56	1.0	6.4	6.33	18.50	0.84	31.8	0.27
	3.170	5.21	1.0	6.5	5.17	15.55	0.82	26.7	0.26
	2.750	5.26	1.0	5.7	5.80	13.50	1.06	23.2	0.33
	2.000	4.53	1.0	5.7	5.72	9.80	1.43	16.85	0.45
	1.400	5.37	1.0	5.0	3.65	6.85	1.31	11.8	0.41
	0.867	5.18	1.0	4.0	3.00	4.26	1.74	7.35	0.55
#7	0.292	8.51	1.0	1.9	1.81	1.44	3.12	2.33	0.93
	0.210	8.31	1.0	1.4	1.55	1.03	3.69	1.67	1.11
	0.122	8.18	1.0	0.68	1.22	0.60	6.12	0.97	1.83
	0.058	6.42	1.0	0.23	1.15	0.285	9.96	0.46	2.98
	0.018	6.82	1.0	0.06	0.49	0.089	13.45	0.14	4.03
#8	3.770	7.31	1.4	7.3	8.87	18.45	1.18	27.3	0.33
	2.890	6.38	1.4	7.6	6.43	14.20	1.11	21.0	0.31
	1.720	5.81	1.4	6.5	4.73	8.43	1.37	12.45	0.38
	1.130	6.63	1.4	5.2	4.03	5.50	1.79	8.14	0.50
#9	0.151	5.56	1.2	0.78	2.56	0.62	5.62	1.48	2.32
	0.217	6.18	1.2	0.99	3.13	0.90	4.86	2.15	2.01
	0.302	6.11	1.2	1.3	4.12	1.25	4.54	2.99	1.88
	0.373	6.28	1.2	2.2	3.96	1.55	3.63	3.70	1.50
	0.482	6.95	1.2	2.6	4.55	2.00	3.15	4.78	1.30
	0.565	6.84	1.2	2.8	5.06	2.34	2.98	5.60	1.23

$$Sc = \frac{\nu}{D} = 1.25 \times 10^5$$

TABLE 4

EXPERIMENTAL VALUES FOR THE

EQUATION $j = Be\ Re^{X}$

Test No.	Bed Characteristics			Void Fraction Term		Reynolds number exponent
	height cm	carbon diameter microns	void fraction	Be theorical (Pfeffer)	Be experimental	
1	8.60	987	0.345	3.8	4.3	-0.53
2	8.59	987	0.296	4.3	5.7	-0.66
3	4.20	248	0.236	5.1	4.8	-0.57
4	7.50	248	0.277	-	-	-
5	12.40	987	0.330	3.9	4.6	-0.58
6	25.20	987	0.315	4.1	4.1	-0.64
7	25.20	987	0.299	4.3	4.1	-0.57
8	25.20	987	0.278	4.5	4.1	-0.50
9	12.40	550	0.413	3.3	4.4	-0.54

within the column. For gas flow in packed beds, saturation is nearly complete when the gas has passed a number of particles of the order of 10 (Thoenes, Kramers, 1958). One can also expect saturation of the first carbon particles of a packed bed with viruses. In this part of the column, the equilibrium concentration is equal to the concentration of viruses in the bulk flow, and the equilibrium concentration will vary in the direction of flow. The log-mean driving force (Equation 17), therefore, is an improper representation of the concentration profile. A second deficiency in the filtration model is that less than 100 percent particle attachment will result in values less than theoretically predicted. Both particle attachment and desorption are interesting aspects of the basic filtration model and merit further investigation by researchers in this field.

Virus removal is a function of void volume, and close correlation between different void volumes is obtained with Pfeffer's parameter Be (Table 4). Experimental data were plotted according to Pfeffer (1964), and the equation of best fit determined by the method of least squares (Figure 3).

$$j = 1.71\ (N_{Re})^{-0.55} \qquad (18)$$

The dependence of Colburn factor on void fraction is also examined according to Grupta and Thodos (1962). They recommend the correlation of $j\epsilon$ to Reynolds number. Wilson and Geankoplis (1966) used this correlation for Reynolds numbers of 0.0016 to 55 and recommend the following equation:

$$j\epsilon = 1.09(Re)^{-2/3} \qquad (19)$$

From Figure 4 the experimental equation is:

$$j\epsilon = 1.50(Re)^{-0.59} \qquad (20)$$

By correcting each test for void fraction by Pfeffer's method and $1/\epsilon$, the Colburn factor was found to vary with Reynolds number to the exponents of -0.55 and -0.59, respectively. McCune and Wilhelm (1949) obtained an exponent of -0.58 for liquid phase mass transfer. The removal of viruses by packed beds correlates well with the simple version of the mass transfer theory used. Additional research, however, is needed to examine the back pressure due to desorption of viruses from the bed. This phenomenon appears to be significant since Colburn factor, j, varies with bed height.

For column heights of 7.50 to 12.40 cm., very good correlation was obtained with Equation 19. The experimental equation for these columns is

$$j\epsilon = 1.72(Re)^{-0.65} \qquad (21)\ \text{(Figure 5)}$$

For column heights of 25.40 cm., the best line through the data yielded the equation

$$j\epsilon = 1.30(Re)^{-0.53} \qquad (22)\ \text{(Figure 6)}$$

Shorter columns gave j values 30 percent higher than the long columns. The Reynolds number exponent is also closer to the theoretical - 2/3 for the shorter columns.

Wilson and Geankopis (1966) report j values to be 15 percent higher for short columns compared to long columns. Bradshaw and Meyers (1963) found j values 40 percent less for

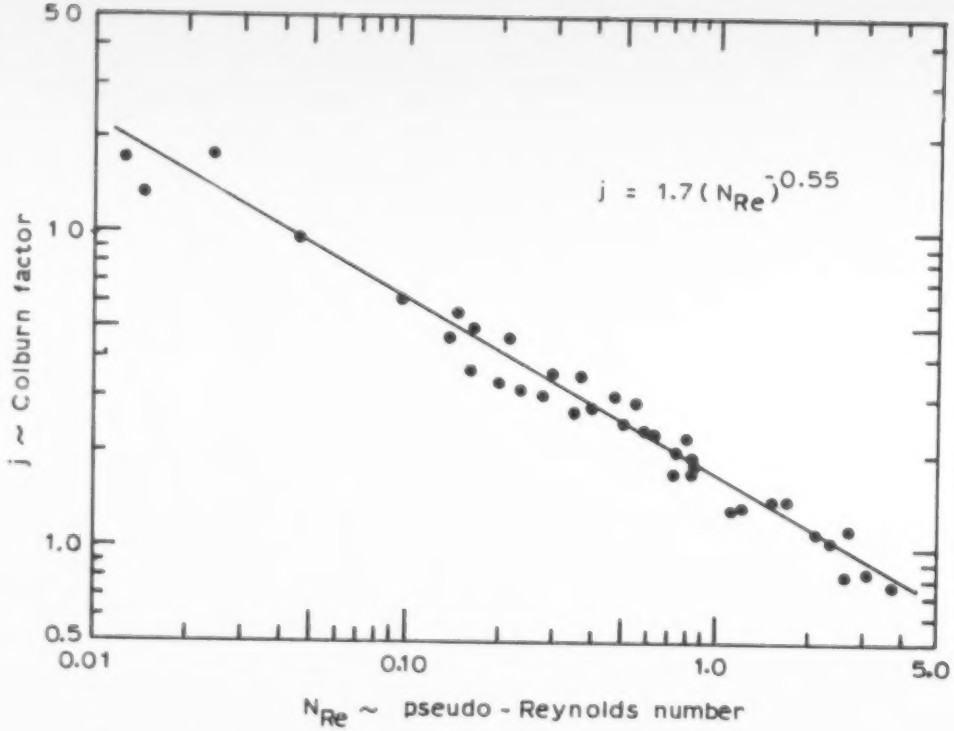

Figure 3. Colburn factor versus Pfeffer's pseudo - Reynolds number

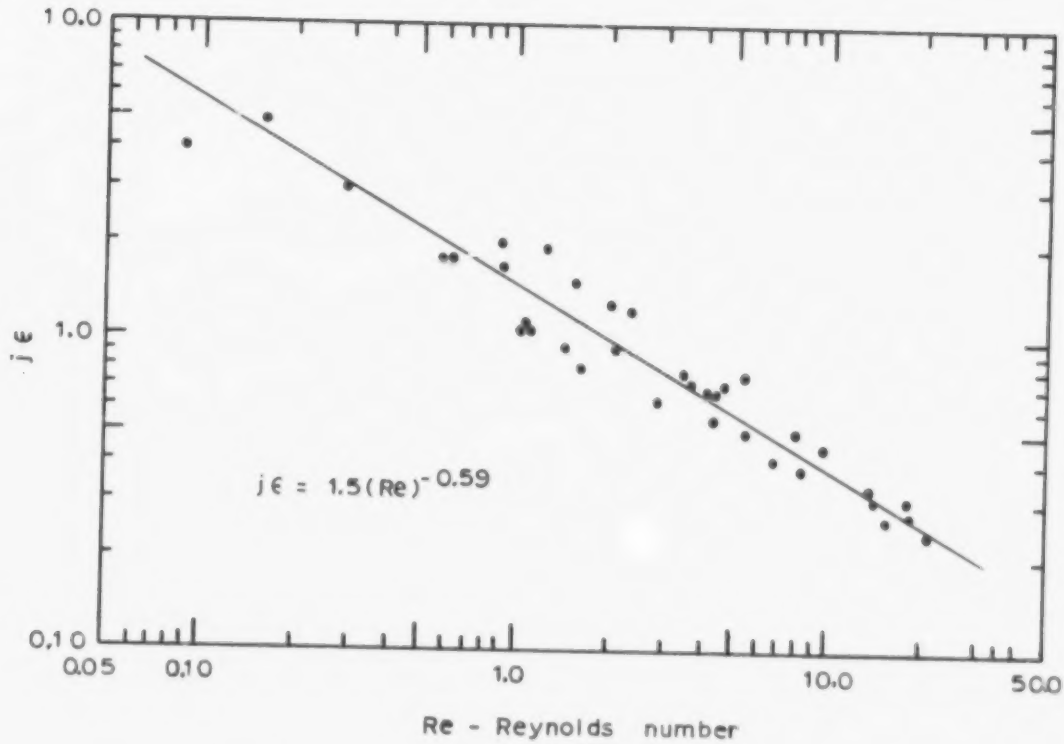

Figure 4. Plot of jϵ vs. Reynolds number

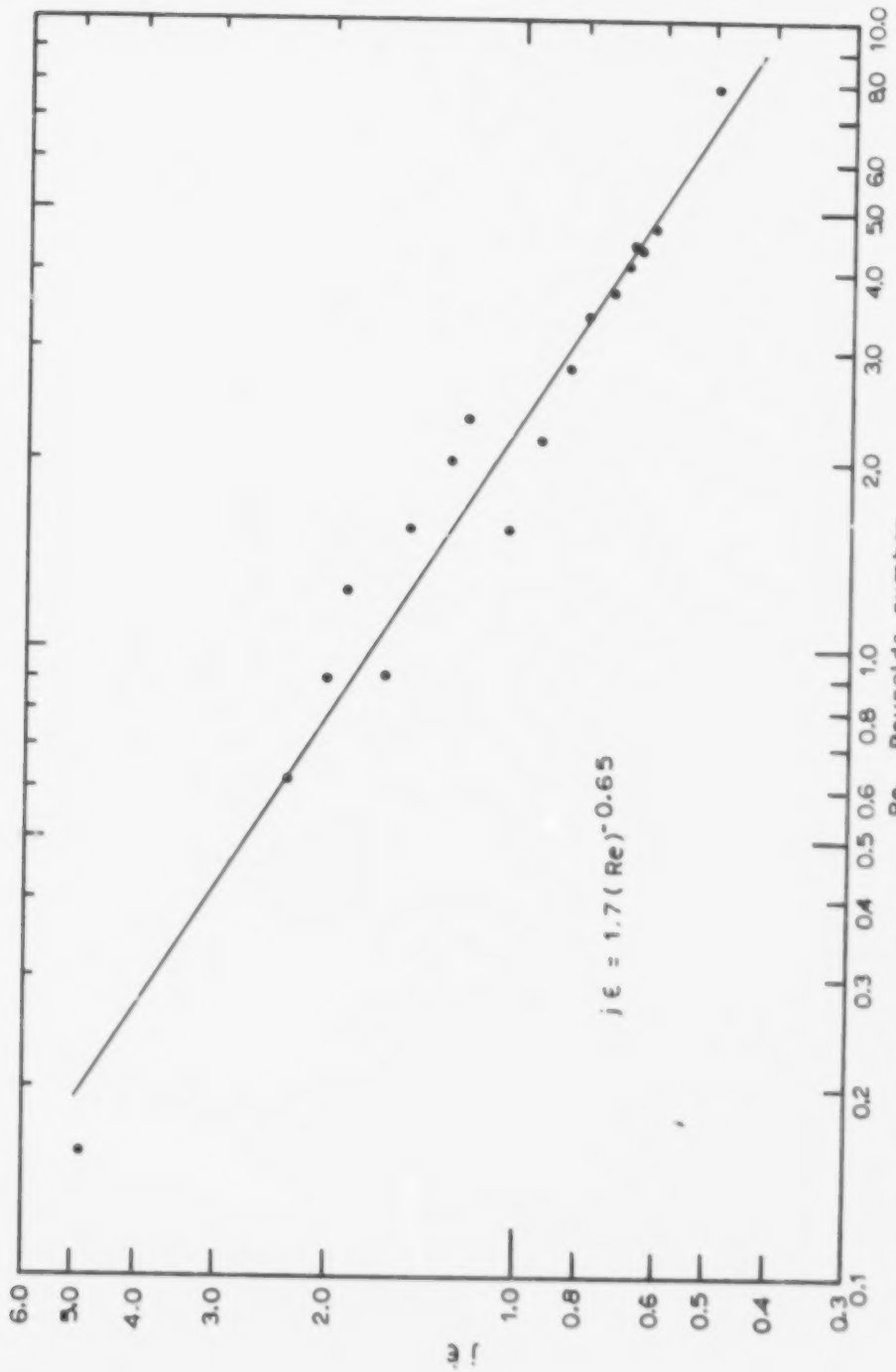

Figure 5. Plot of jε vs. Reynolds number for column heights of 7.5 to 12.4 cm.

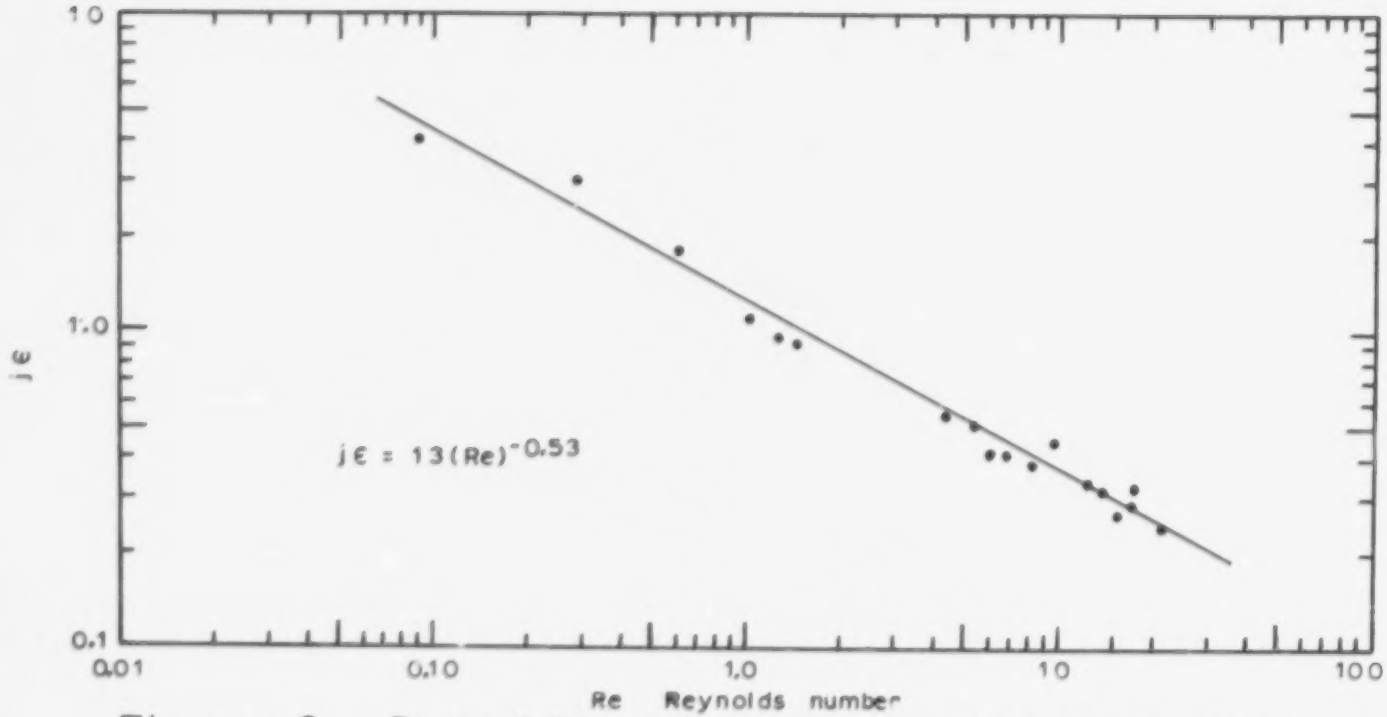

Figure 6. Plot of jε vs. Reynolds number for column heights of 25.4 cm.

gases in 4-inch beds compared to 1-inch beds. They concluded that j was independent of bed height if the mean driving force used for the longer lengths was obtained by graphical integration, using the outlet concentrations from the shorter lengths.

In activated carbon adsorption columns and sand filters, the concentration gradient and mean driving force may differ from the log mean driving force, ΔC_{lm}. Both the equilibrium concentration and mean driving force will vary with degree of saturation of the bed. This particular problem should be examined by determining the concentration profile in the bed based upon isothermal adsorption. This discussion indicates the need for getting internal samples, so that the true concentration gradient and mean driving force can be determined.

Conclusion

In summary, under optimum adsorption conditions, virus removal in packed beds of activated carbon closely followed mass transfer theory. Colburn factor, j, varied with fractional void volume of the bed, but j was constant if the void fraction corrections of Pfeffer and of $1/\epsilon$ were applied. Colburn factor also varied with bed heights. Greater deviation from theoretical equations occurred with longer column heights. This phenomenon is probably due to improper representation of the concentration profile through the column.

From this study, it appears that the particle transport mechanism in filtration can be described by application of the mass transfer theory when diffusion is the limiting process for removal. Application of mass transfer with information on isothermal adsorption may eliminate the effect of column height.

Nomenclature

Am	=	surface area per unit volume of packing, $cm.^2$ per $cm.^3$
Be	=	constant depending on void fraction
C_1	=	inlet concentration, viruses per $cm.^3$
C_2	=	exit concentration, viruses per $cm.^3$
ΔC_{lm}	=	log mean concentration, viruses per $cm.^3$
C^*	=	equilibrium concentration, viruses per $cm.^3$
D	=	diffusion coefficient, $cm.^2$ per sec.
Dm	=	mean effective diameter of bed particles, cm.
G	=	flow rate, $cm.^3$ per sec.
g	=	gravitational constant, cm. per $sec.^2$
j	=	dimensionless Colburn factor
k	=	transfer coefficient, cm. per sec.
L	=	bed height, cm.
N_{Re}	=	pseudo-Reynolds number defined by $[1 - (1 - \epsilon)^{5/3}/W]^{-1/2}Re$
Pe	=	dimensionless Péclet number, Re x Sc
ΔP	=	pressure drop, gm. per $cm.^2$
Re	=	dimensionless Reynolds number, uDm/ν
Sc	=	dimensionless Schmidt number, ν/D
Sh	=	dimensionless Sherwood number, kDm/D
Sv	=	specific surface area, $cm.^2$ per $cm.^3$
u	=	superficial velocity based on empty column, cm. per sec.
U	=	mass flow rate of fluid, $U = \rho_1 u$, gm. per $cm.^2$ sec.

Nomenclature (cont'd)

V = volume of column, cm.^{3}

W = function of γ , $W = 2 - 3\gamma + 3\gamma^5 - 2\gamma^6$

Greek Symbols

γ = ratio of inner sphere to outer sphere radii, dimensionless

ϵ = fractional void volume, dimensionless

ρ = particle density, gm. per cm.^{3}

ρ_B = bulk density, gm. per cm.^{3}

ρ_l = liquid density, gm. per cm.^{3}

μ = absolute viscosity, gm. per cm. sec.

ν = kinematic viscosity, cm.^{2} per sec.

Literature Cited

Bradshaw, R. D., Myers, J. E., A.I.Ch.E. Journal, 9. 590 (1963).

Cookson, J. T., North, W. J., Environ. Sci. Technol. 1, 46 (1967).

Edwards, D. M., Monke, E. S., J. Am. Water Works Assoc. 59, 1310 (1967).

Ergun, S., Anal. Chem. 23, 151 (1951).

Friedlander, S. K., Ind. Eng. Chem. 50, 1161 (1958).

Gupta, A. S., Thodos, G., A. I. Ch. E. Journal, 8, 608 (1962).

Ives, K. J., Gregory, J., Proc. Soc. for Water Treatment and Examination, 15, 93, (1966).

Ives, K. J., Sholyi, I., Journal Sanitary Engineering Division, ASCE. 91, 1 (1965)

Jorden, R. M., J. Am. Water Works Assoc. 55, 771 (1963).

McCune, L. K., Wilhelm, R. H., Ind. Eng. Chem. 41, 1124 (1949).

O'Melia, C. R., Crapps, D. K., J. Am. Water Works Assoc., 56, 1326 (1964).

O'Melia, C. R., Stumm, W., J. Am. Water Works Assoc. 59, 1393 (1967).

Pfeffer, R., I. & E. C. Fundamentals, 3, 380 (1964).

Pfeffer, R., Happel, J., A. I. Ch. E. Journal, 10, 605 (1964).

Robeck, G. G., Project Report, Robert A. Taft Sanitary Engineering Center, May 1963.

Theones, D., Kramers, H., Chem. Eng. Sci. 8, 271, (1958).

Wilson, E. J., Geankoplis, C. J., I & EC Fundamentals, 5, 9 (1966).